Martin Marietta Laboratories

MARTIN MARIETTA

(2)

CONTACT FORMATION ON (HG, CD)TE

FINAL REPORT

W.A. BECK AND G.D. DAVIS

DECEMBER 1989

U.S. ARMY RESEARCH OFFICE

CONTRACT: DAAG29-85-C-0023

MARTIN MARIETTA LABORATORIES
1450 SOUTH ROLLING ROAD
BALTIMORE, MARYLAND 21227

UNCLASSIFIED
SECURITY CLASSIFICATION OF THIS PAGE

MASTER COPY - FOR REPRODUCTION PURPOSES

REPORT DOCUMENTATION PAGE

1a. REPORT SECURITY CLASSIFICATION Unclassified	1b. RESTRICTIVE MARKINGS
2a. SECURITY CLASSIFICATION AUTHORITY	3. DISTRIBUTION/AVAILABILITY OF REPORT Approved for public release; distribution unlimited.
2b. DECLASSIFICATION/DOWNGRADING SCHEDULE	
4. PERFORMING ORGANIZATION REPORT NUMBER(S) MML TR 89-117C	5. MONITORING ORGANIZATION REPORT NUMBER(S) ARO 21077.8-MS
6a. NAME OF PERFORMING ORGANIZATION Martin Marietta Laboratories 6b. OFFICE SYMBOL (If applicable)	7a. NAME OF MONITORING ORGANIZATION U. S. Army Research Office
6c. ADDRESS (City, State, and ZIP Code) 1450 South Rolling Road Baltimore, Maryland 21227	7b. ADDRESS (City, State, and ZIP Code) P. O. Box 12211 Research Triangle Park, NC 27709-2211
8a. NAME OF FUNDING/SPONSORING ORGANIZATION U. S. Army Research Office 8b. OFFICE SYMBOL (If applicable)	9. PROCUREMENT INSTRUMENT IDENTIFICATION NUMBER DAAG29-85-C-0023
8c. ADDRESS (City, State, and ZIP Code) P. O. Box 12211 Research Triangle Park, NC 27709-2211	10. SOURCE OF FUNDING NUMBERS PROGRAM ELEMENT NO. / PROJECT NO. / TASK NO. / WORK UNIT ACCESSION NO.
11. TITLE (Include Security Classification) Contact Formation on (Hg,CD)Te (u)	
12. PERSONAL AUTHOR(S) W.A. Beck and G.D. Davis	
13a. TYPE OF REPORT Final	13b. TIME COVERED FROM Aug. 85 TO Nov. 89
14. DATE OF REPORT (Year, Month, Day) 1989 December 21	15. PAGE COUNT 73
16. SUPPLEMENTARY NOTATION The view, opinions and/or findings contained in this report are those of the author(s) and should not be construed as an official Department of the Army position, policy, or decision, unless so designated by other documentation.	

17. COSATI CODES			18. SUBJECT TERMS (Continue on reverse if necessary and identify by block number)
FIELD	GROUP	SUB-GROUP	contact, HgCdTe, noise, surfaces, interfaces, metal

19. ABSTRACT (Continue on reverse if necessary and identify by block number)

The interactions between both cleaved and ion-sputtered (HgCd)Te and deposited overlayers that were investigated under ARO contract DAAG29-85-C-0023 are reviewed and compared to those reported by others. The overlayers are classified into four groups - ultrareactive, reactive, intermediate reactive, and unreactive - based on the relative heats of formation of the overlayer telluride and HgTe and CdTe. Ultrareactive overlayers react with both HgTe and CdTe to form an interfacial metallic telluride and elemental Hg and Cd, which are lost from the interface, whereas unreactive overlayers react only with the HgTe component. Once the HgTe is depleted from the surface region, further deposition results in growth of a metallic film. Unreactive metals, on the other hand, do not react with

20. DISTRIBUTION/AVAILABILITY OF ABSTRACT ☐ UNCLASSIFIED/UNLIMITED ☐ SAME AS RPT. ☐ DTIC USERS	21. ABSTRACT SECURITY CLASSIFICATION Unclassified
22a. NAME OF RESPONSIBLE INDIVIDUAL	22b. TELEPHONE (Include Area Code) / 22c. OFFICE SYMBOL

DD FORM 1473, 84 MAR

83 APR edition may be used until exhausted.
All other editions are obsolete.

SECURITY CLASSIFICATION OF THIS PAGE
UNCLASSIFIED

the surface, but form a stoichiometric interface. In contrast, the extent of interactions between intermediate overlayers and (HgCd)Te depend on other factors, including the stability or reactivity of the surface and substrate material, the heats of cation alloying, and the propensity of the overlayers element to diffusion into the (HgCd)Te. The use of thin interlayers can substantially alter the interfacial behavior, however. They can either increase or decrease the indiffusion of the overlayer material into the (HgCd)Te. They can also change the overlayer morphology and control the band bending near the surface.

The resistance and 1/f noise of Au and Al contacts to ion-sputtered p-type $Hg_{0.79}Cd_{0.21}Te$ and of Ge contacts to $Hg_{0.7}Cd_{0.3}Te$ were measured at temperatures of 12, 40, 77, and 295K. The Au and Al contacts were ohmic at all temperatures, whereas the Ge contacts were partially rectifying. The specific contact resistance for Au and Al varied by about a factor of ten up to $9 \times 10^{-4} \Omega cm^{-2}$ and $2 \times 10^{-3} \Omega cm^2$, respectively, at 295K, and there was little variation in resistance down to 12K. The 1/f noise of the Au and Al contacts could be described as a power spectral density of resistance fluctuations, S_R, which varied with the contact diameter, d, as $S_R \propto d^{-m}$, where $5 \leq m \leq 6$ for Au and $2 \leq m \leq 3$ for Al. The values of m suggest that whereas the 1/f noise of the Au contacts originated at the 1/f (HgCd)Te interface or in the underlying (Hg,Cd)Te, the 1/f noise of the Al contacts originated in a surface conduction layer next to the contact. The magnitude of the 1/f noise was significantly larger than expected for any fundamental 1/f noise source.

CONTACT FORMATION ON (HG,CD)TE

FINAL REPORT

W.A. BECK AND G.D. DAVIS

DECEMBER 1989

U.S. ARMY RESEARCH OFFICE

CONTRACT DAAG29-85-C-0023

MARTIN MARIETTA LABORATORIES
1450 SOUTH ROLLING ROAD
BALTIMORE, MD 21227

Contents

List of Figures

I. INTRODUCTION

Ohmic contacts are an important part of (Hg,Cd)Te infrared detectors. To achieve high sensitivity in staring detectors it is important that the noise be low at frequencies above the video frame rate. Low contact resistance is important both for high-frequency heterodyne detectors, where the resistance may determine the RC time constant of the detector, and for lower-frequency photodiodes because the 1/f noise of the diode junction strongly depends on the junction bias. If the contact resistance is too high, the operating bias on the detector shifts with changing photocurrent, so that even if the junction is optimally biased when looking at one scene, it is improperly biased when looking at a different scene, resulting in excess 1/f noise.

Surface-sensitive measurements during overlayer growth on many semiconductors have shown that defects in the semiconductor induced by the metal strongly influence the electron transport between the two materials.[1-4] These defects can be caused by such processes as chemical reactions, indiffusion of the contact metal, and outdiffusion of the semiconductor components and generally involve decomposition of the semiconductor near the interface. They are especially important during interactions between reactive metals and semiconductors with low thermodynamic stability, such as (Hg,Cd)Te.

The low thermodynamic stability of (Hg,Cd)Te is largely due to the weakness of the Hg-Te bond and the dissimilarity between the Hg and Cd atomic states.[5-7] These characteristics lead to the adjustable nature of the bandgap, but are also responsible for the ease of creation and the mobility of defects and the decreased stability of the already thermodynamically weak HgTe alloy component.[8,9]

The results of this program and those of similar investigations by Stanford University/Santa Barbara Research Center and University of Minnesota/McDonnell Douglas

show that the defect mechanisms discussed above for metal-semiconductor interactions in general are especially important for (HgCd)Te. Overlayers can be grouped into four classes[10,11] –ultrareactive, reactive, intermediate, and unreactive–based on the relative heats of formation of the respective tellurides[8,9] (Fig. 1). The ultrareactive group, which includes Ti,[12] Sm,[13] and Yb,[14] form tellurides that are more stable than CdTe, whereas the reactive class of overlayers, such as Al,[15–19] In,[16,17] and Cr,[20–22] form tellurides with heats of formation between those of HgTe and CdTe. At the other extreme of reactivity are the unreactive overlayers (Au[23,24] and Sb[25]) that form tellurides even less stable than HgTe. Finally, the last group of overlayers, those with intermediate reactivity, induce behavior intermediate between that of reactive and unreactive metals.[26] They include those elements whose tellurides possess heats of formation close to that of HgTe, such as Ge,[26,27] Ag,[18,19,26,28] Cu,[19,26,29] and Pt.[30] For these elements, because the energetics of interfacial reactions are small, the behavior of the interface can depend on other factors, including surface preparation, sample history, heats of cation alloying, and propensity of the overlayer element to diffuse into the semiconductor.

In this report, each of these classes of overlayers are illustrated with one or more examples. The effects, if any, of substrate surface preparation and material quality are also shown. We also report on limited results using interlayers to control interfacial behavior.[25,31] For more details, the original publications should be consulted.

Electrical measurements on contacts to (Hg,Cd)Te are less extensive. Pawlikowski measured the resistance of an assortment of metal contacts to n- and p-type (Hg,Cd)Te that had been polished and etched.[32,33] He inferred that the electrical properties of the contacts are strongly influenced by interface states[34] and that the n-type layer that often appears on p-type (Hg,Cd)Te plays an important role in the final electrical properties of the contact.[35] Photo-effect measurements[36] on Au and In contacts to n-type $Hg_{0.825}Cd_{0.175}Te$ indicated barrier heights on the order of 0.3 eV, even though the contacts were ohmic. The barriers were attributed to a high density of interface states.

1/f noise is a widely observed phenomena in which the power spectral density of the fluctuating quantity, e.g., voltage or current, is approximately proportional to the inverse of the measurement frequency. In the case of electrical 1/f noise in resistive samples it is almost always observed that the power spectral density of the current or voltage fluctuations is proportional to the square of the current through the sample,

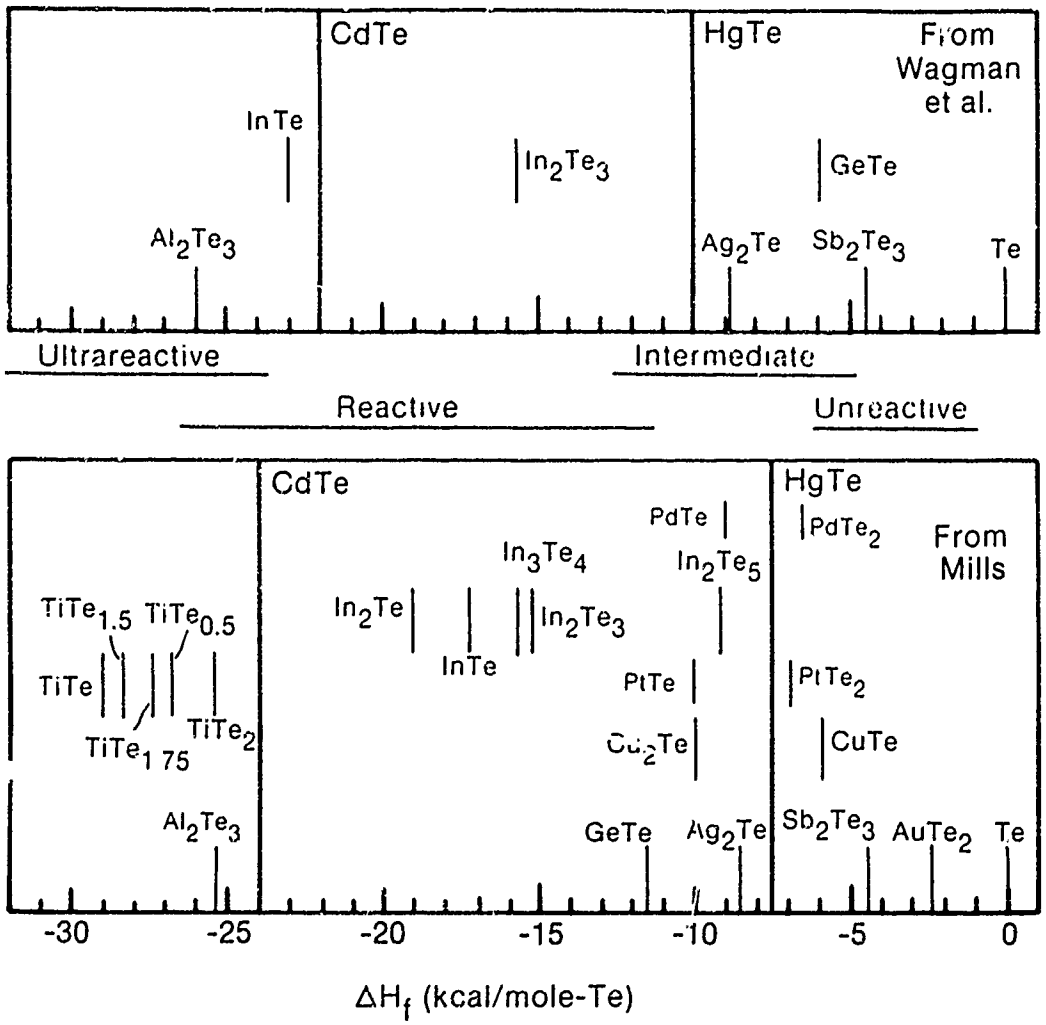

Figure 1: Heats of formations of selected tellurides from Mills[8] and Wagman et al.[9] (adapted from ref. 10).

which indicates that the noise is due to a fluctuation in the *resistance* of the sample. Hooge found[37] that the noise from homogeneous samples carrying a homogeneous current could often be described by

$$\frac{S_I(f)}{I^2} = \frac{S_R(f)}{R^2} = \frac{\alpha_H}{fN} \tag{1}$$

where I is the current, R is the resistance, S_I and S_R are the respective power spectral densities, N is the number of carriers in the sample, and α_H is the Hooge parameter. For the case of current flow away from a small contact, wherein the current is not homogeneous, Hooge applied Eq. (1) to thin hemispherical shells and summed the noise from the shells to obtain

$$\langle(\Delta R/R)^2\rangle = \frac{4\alpha\pi^2}{5\rho^2 n} R^3 \frac{\Delta f}{f}, \tag{2}$$

where ρ is the resistivity of the substrate material and n is the carrier density. Equation (2) (with $\alpha_H = 2 \times 10^{-3}$) adequately describes the resistance (and therefore diameter) dependence of many metal-to-metal contacts, indicating that the noise in those contacts is not a surface effect, but rather a manifestation of bulk 1/f noise within the restricted volume under the contact.

An excellent review of the physical significance of the Hooge parameter, α_H, was recently published by van der Ziel.[38] There are two classes of 1/f noise for which α_H can be calculated from physical processes. The first, *fundamental* 1/f noise, was first proposed by Handel[39,40] and is thought to be a direct result of perturbation of the electron wave function by the Bremsstrahlung emission that occurs in any scattering event. The predicted value of α_H has an upper limit of 3.1×10^{-3}, but can be much less, depending on the scattering mechanism. Handel also proposed a somewhat different fundamental mechanism called "coherent state" 1/f noise, for which $\alpha_H = 4.6 \times 10^{-3}$. The noise is termed "fundamental" because it is unavoidably linked with the collisions that control transport through the material.

Nonfundamental 1/f noise, on the other hand, involves diffusion of defects or carrier trapping and release by traps in a conducting channel, space-charge region, or surface oxide. The magnitude of the noise depends on the density of the traps such that the effective α_H can vary from zero up to values much larger than the 4.6×10^{-3} limit for fundamental noise.

Several studies of 1/f noise in (Hg,Cd)Te photodiodes have been reported. The noise was associated with surface leakage currents near the p-n junction,[41,42] with bulk

band-to-band tunneling current,[43] or with the fundamental coherent-state mechansism.[44] Despite the fact that none of the studies found that the device ohmic contacts played a dominant role in generating 1/f noise, that conclusion could change if smaller contacts are used. Moreover, since defects play such an important role in determining the amount of nonfundamental 1/f noise, it would be useful to correlate the dramatic chemical interactions seen at the metal/(Hg,Cd)Te interface with the 1/f noise produced at or near those interfaces.

The goal of this program was to measure the chemical interactions that take place at the metal/(Hg,Cd)Te interface and to correlate those interactions with the electrical properties of the contacts. The interfacial chemistry measurements were completed for a wide range of contact metals and have lead to a classification scheme for the metals based on their heat of formation of compounds with Hg, Cd, and Te. Electrical measurements were completed on Au, Al, and Ge contacts to ion-sputtered materials, including the first systematic measurement of 1/f noise in these contacts. In addition, contacts were formed to vacuum-cleaved surfaces, but these samples could not be measured due to the loss of the final 6-month funding increment.

II. SURFACE ANALYSIS

A. EXPERIMENTAL PROCEDURE

Investigation of each of the metal-(HgCd)Te interfaces discussed here were made using photoelectron spectra of the surface following deposition of increasing amounts of the overlayer material. The details are given in the original publications.[10–31] In most cases, the substrate was (HgCd)Te cleaved in situ along the (110) face. In the others, the surface had a random orientation and was sputtered with Ar^+ ions prior to deposition.

Some of the data have been converted to atomic compositions and displayed on surface behavior diagrams (SBDs).[26,45–47] These diagrams allow the composition of the semiconductor to be traced during the deposition process and provide a convenient means to visually compare the behavior induced by the different overlayers or exhibited by different substrates.

B. RESULTS AND DISCUSSION

1. Single Overlayers

Reactive and ultrareactive overlayers

Photoelectron spectra of cleaved (HgCd)Te before and after deposition of the reactive metal Al are presented in Fig. 2.[16] They clearly indicate that very small

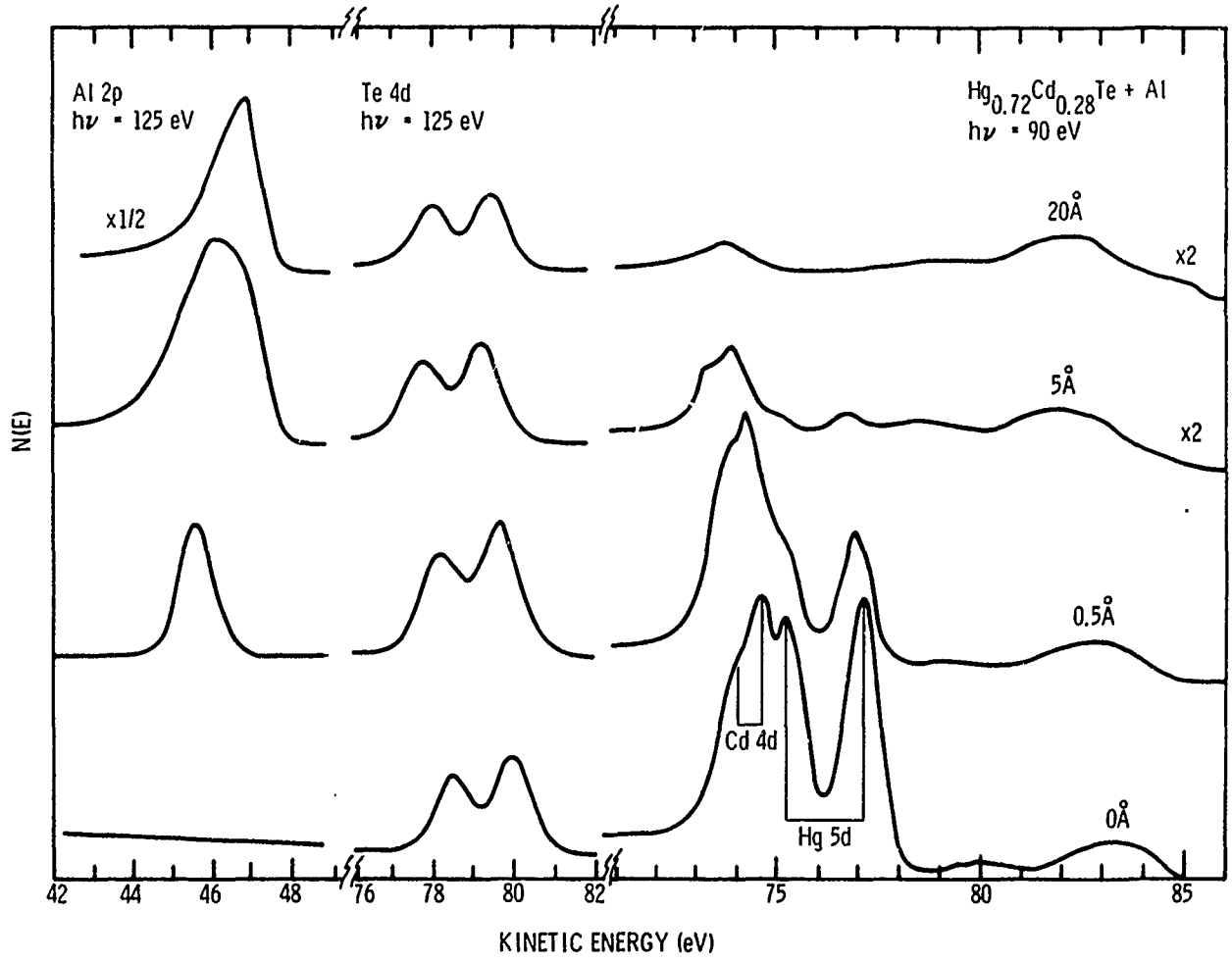

Figure 2: Valence band and core level spectra from cleaved (HgCd)Te as a function of Al coverage.[16]

amounts of Al induce dramatic changes in the (HgCd)Te surface chemistry. The most obvious of these is a rapid decrease in the amount of Hg present in the surface region, with the Hg/Cd ratio decreasing to 20% of its initial value with the deposition of only 1 Åof Al (one monolayer of Al corresponds to 1.12 Å) and remaining at this value at higher coverages.[16] Figure 2 also indicates a persistence of the Te signal, a growth of the Al peak with an evolution from one chemical state to another, and a shift of the spectral features to 0.6 eV lower kinetic energy. The initial Al peak corresponds to Al_2Te_3 as a result of the exchange reaction

$$3HgTe + 2Al \rightarrow Al_2Te_3 + 3Hg \quad (3)$$

while the second peak corresponds to metallic Al. This state, which is first seen at 2 Å, grows until it dominates the spectrum at high coverages.

The evolution of the surface chemistry is best seen in the HgTe-CdTe-Al_2Te_3-Al SBD of Fig. 3 and, neglecting the Al contribution, in the Hg-Cd-Te SBD of Figure 4. In the HgTe-CdTe-Al_2Te_3-Al SBD, the C-shaped evolutionary path begins along the HgTe-CdTe axis at the point corresponding to $Hg_{0.72}Cd_{0.28}Te$. During the initial stages of deposition, the surface composition travels along an iso-[CdTe] line, indicating that the Al_2Te_3 is replacing the HgTe in the near surface region in accordance with reaction 3, but is not replacing or overlaying the CdTe. (That is, the exchange reaction

$$3CdTe + 2Al \rightarrow Al_2Te_3 + 3Cd \quad (4)$$

is not proceeding.) Once the near-surface HgTe is depleted and the freed Hg has left the interface, a metallic Al overlayer begins to grow and the composition evolves toward the Al_2Te_3-Al axis. At this point, the semiconductor is barely detected by the measurement, but Te diffuses to the surface. As the overlayer thickens further, metallic Al becomes an increasingly larger fraction of the detection volume.

A complementary view of the interface is shown in the Hg-Cd-Te SBD of Fig. 4 which also contains equivalent results following deposition onto sputtered substrates. The data from the cleaved substrates again begin at the point corresponding to $Hg_{0.72}Cd_{0.28}Te$ and follow a bowed path between the two model evolutionary lines. (The first of these lines, pointing directly toward the Te vertex, is the evolutionary path corresponding to outdiffusion of Te with no change in the relative Hg and Cd concentrations. The second, pointing directly away from the Hg vertex, is the evolutionary path corresponding to a loss of Hg from the interfacial region with no

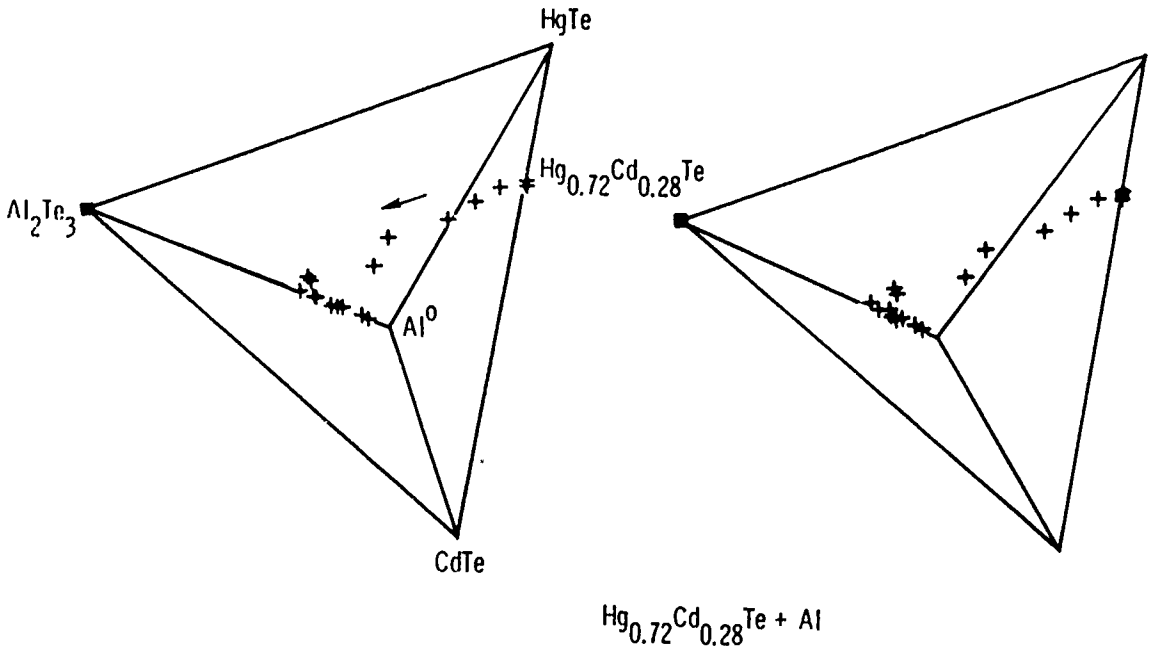

Figure 3: HgTe-CdTe-Al_2Te_3-Al SBD showing the evolution of the surface composition upon Al deposition.[16] The surface composition traces a C-shaped path beginning on the HgTe-CdTe axis and ending near the Al vertex. (The two views of the SBD are rotated by 7°. A three-dimensional image can be obtained by viewing them through a stereo viewer.)

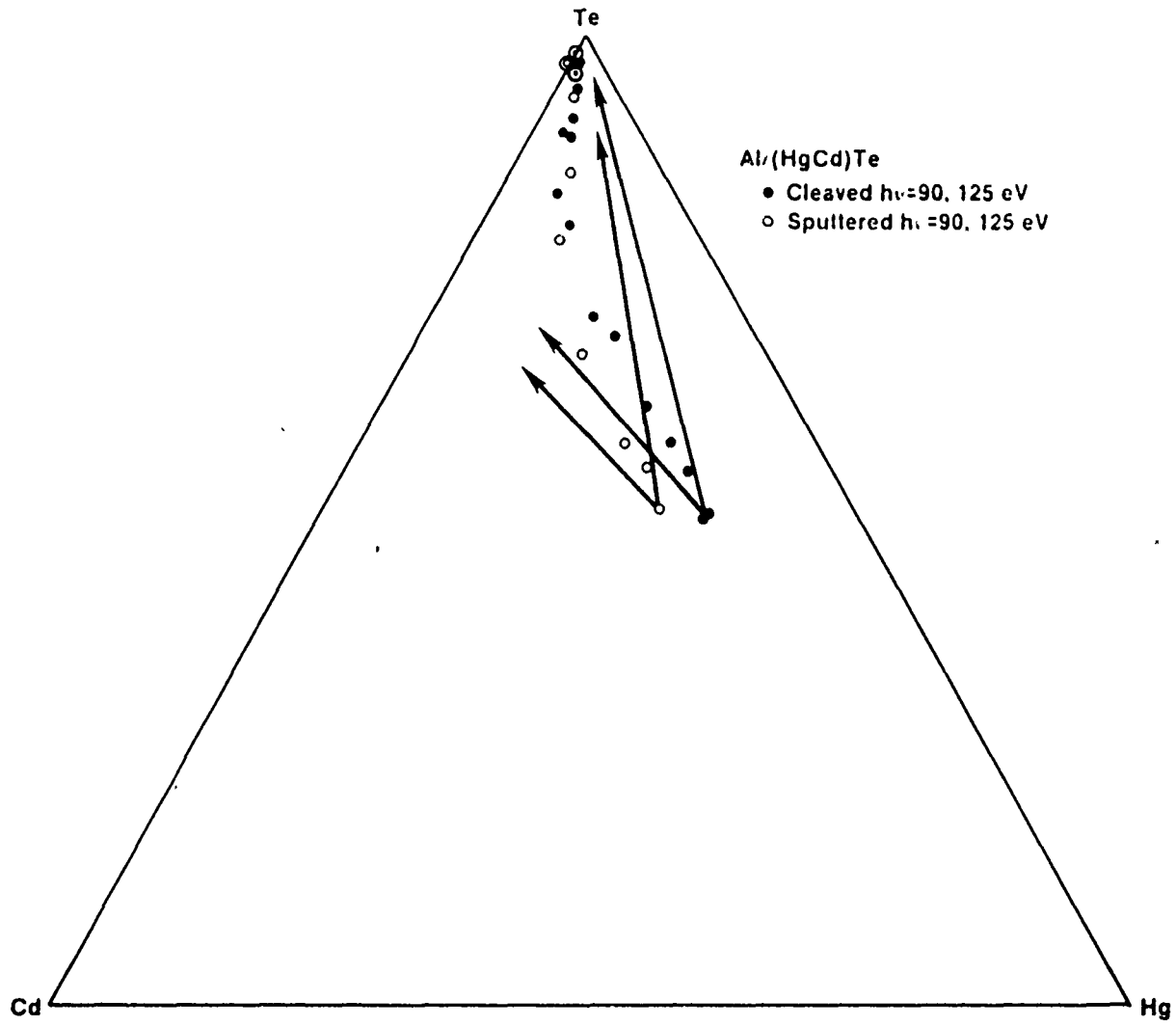

Figure 4: Hg-Cd-Te SBD illustrating the evolution of the semiconductor-component composition during Al deposition onto both cleaved and sputtered substrates. Points representing the deposition of 10-20 Åcircled. (Data are from Refs. 16 and 17).

outdiffusion or, alternatively, equal outdiffusion of Cd and Te. A third possible evolutionary path, representing either a stoichiometric interface with no outdiffusion or a stoichiometric interface with indiffusion of the overlayer material, would be a constant semiconductor-component composition.[26]) The course of the data is a combination of the first two model paths and again demonstrates the outdiffusion of Te and the loss of Hg from the interfacial region.

An equivalent path is taken by the sputtered substrate despite its different starting composition, caused by the preferential sputtering of Hg from the semiconductor.[17,18-51] This similarity in behavior is also reflected by identical Hg/Cd ratios (normalized to that of the clean surface) exhibited by substrates with the two surface preparations.[10,17]

Deposition of other reactive metals, In onto cleaved[16,17] and sputtered[17] substrates and Cr onto cleaved substrates,[20-22] result in similar behavior to deposition of Al[15-19] with a dramatic loss of Hg from the interface region. Based on these results, a model has been developed to explain the interactions between (HgCd)Te and reactive overlayers. During the initial stages of deposition, the metal reacts with the HgTe semiconductor component on the surface, in accordance with reaction 3, to form a metal telluride and elemental Hg, which leaves the surface. The CdTe component, on the other hand, is inert and remains unchanged. (A small amount may react with Cr.) Some of the metal (in the case of Al and In), and possibly some Hg, diffuses into the semiconductor to act as donors, thus causing the Fermi level to move upward and increasing the inversion of the cleaved surface. (The sputtered surface is already severely inverted due to ion-bombardment-induced defects and any indiffusion does not further increase the band bending.) Once the HgTe is consumed from a thin surface region and is no longer available to the deposited metal, the metal remains in its elemental state. Accompanying the growth of this film is the outdiffusion to the surface of Te that was not trapped at the interface.

The interaction with ultrareactive overlayers, in which both reaction 3 and reaction 4 are predicted to occur, has been less well studied.[12-14] Measurements following thin layers of Ti indicated that both Hg and Cd are being lost from the interfacial region and that the depth and rate of formation of the Hg depletion is much greater than that seen during Al deposition or seen for Cd during the Ti deposition. These increases cannot be explained by the increased net energetics of the exchange reaction, but are apparently related to the loss of Cd, resulting in a complete disruption of the semiconductor lattice and a lack of an inert component to "passivate" the interface.[12]

Unreactive Overlayers

Unreactive overlayers are at the other extreme, compared with ultrareactive materials. They are limited to Au[23,24] and Sb[52] (based on our definitions), which form tellurides even less stable than HgTe. The Hg-Cd-Te SBDs of Figs. 5 and 6 show the evolution of the semiconductor-component composition during Au and Sb deposition, respectively, for both cleaved and sputtered substrates. Two principal differences can be seen between the evolutionary paths of these two elements and that of Al (Fig. 4): the Au and Sb data are closer to the starting composition for a given overlayer thickness and they follow more closely the line toward the Te vertex, indicating little loss of Hg, relative to Cd. For Sb, in fact, there is no decrease in the Hg/Cd ratio up to 20 ÅSb (one monolayer of Sb corresponds to 2.05 Å) for either cleaved or sputtered surfaces, whereas the slight bowedness of the Au evolutionary path indicates a small decrease (20%) of the Hg/Cd ratio for coverages of 10-50 Å[23,24] (one monolayer of Au corresponds to 1.15 Å).

The slow rate of change of the semiconductor-component composition with overlayer thickness, which is particularly notable for Sb, is largely due to the stoichiometric nature of the interface – because reaction 3 does not occur, there is little freed Hg available for escape or Te available for diffusion. However, there is another mechanism that leads to partial dissociation of the semiconductor alloying constituents during Au deposition. This is discussed below.

Although it is not apparent from the SBDs, the signals from the semiconductor components, especially Te, do not attenuate as quickly as expected from an abrupt, uniform overlayer, especially in the case of Au. Two factors probably contribute to this phenomenon. The first is island formation during the deposition. In this case, the substrate signals would attenuate during the very initial stages as if a uniform overlayer were growing; then, as islands nucleated and grew, the substrate signals would persist (but slowly decrease as the islands cover a larger fraction of the surface) until the islands agglomerate. The second factor is alloying of the cations with the overlayer. This has been shown to control the behavior of the Pt-(HgCd)Te interface[30] and is predicted to influence the Au-(HgCd)Te interface as well, but to a lesser degree. In this case, the negative heat of alloying of Cd and Hg in Au would make the dissociation reactions more energetically favorable. Any freed Hg or Cd would then diffuse throughout the overlayer while the freed Te would react with the Au to form $AuTe_2$ and diffuse to the surface. The cation signals then would slowly attenuate as

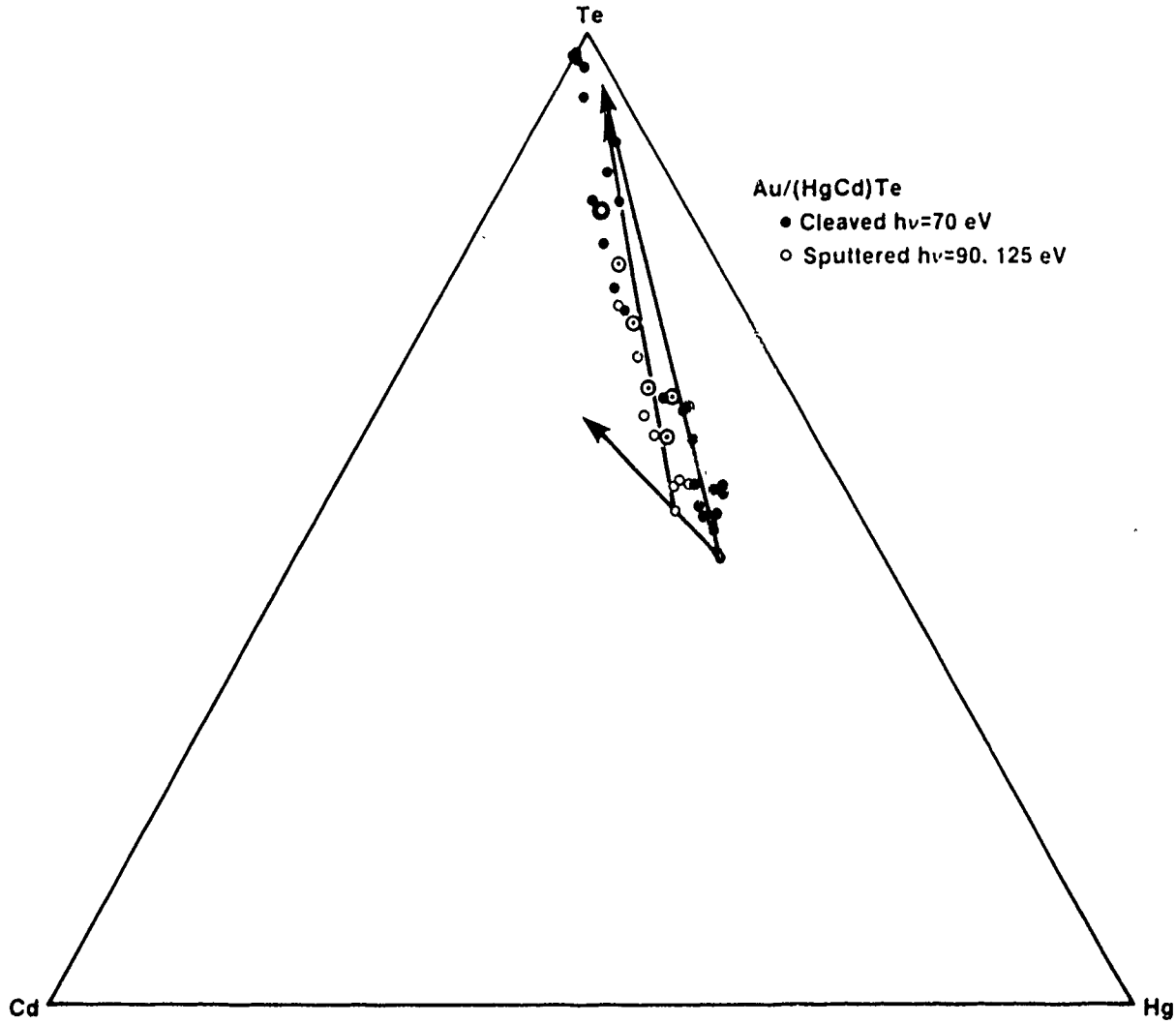

Figure 5: Hg-Cd-Te SBD illustrating the evolution of the semiconductor-component composition during Au deposition onto both cleaved and sputtered substrates. Points representing the deposition of 10-20 Åcircled. (Data are from Refs. 23 and 24).

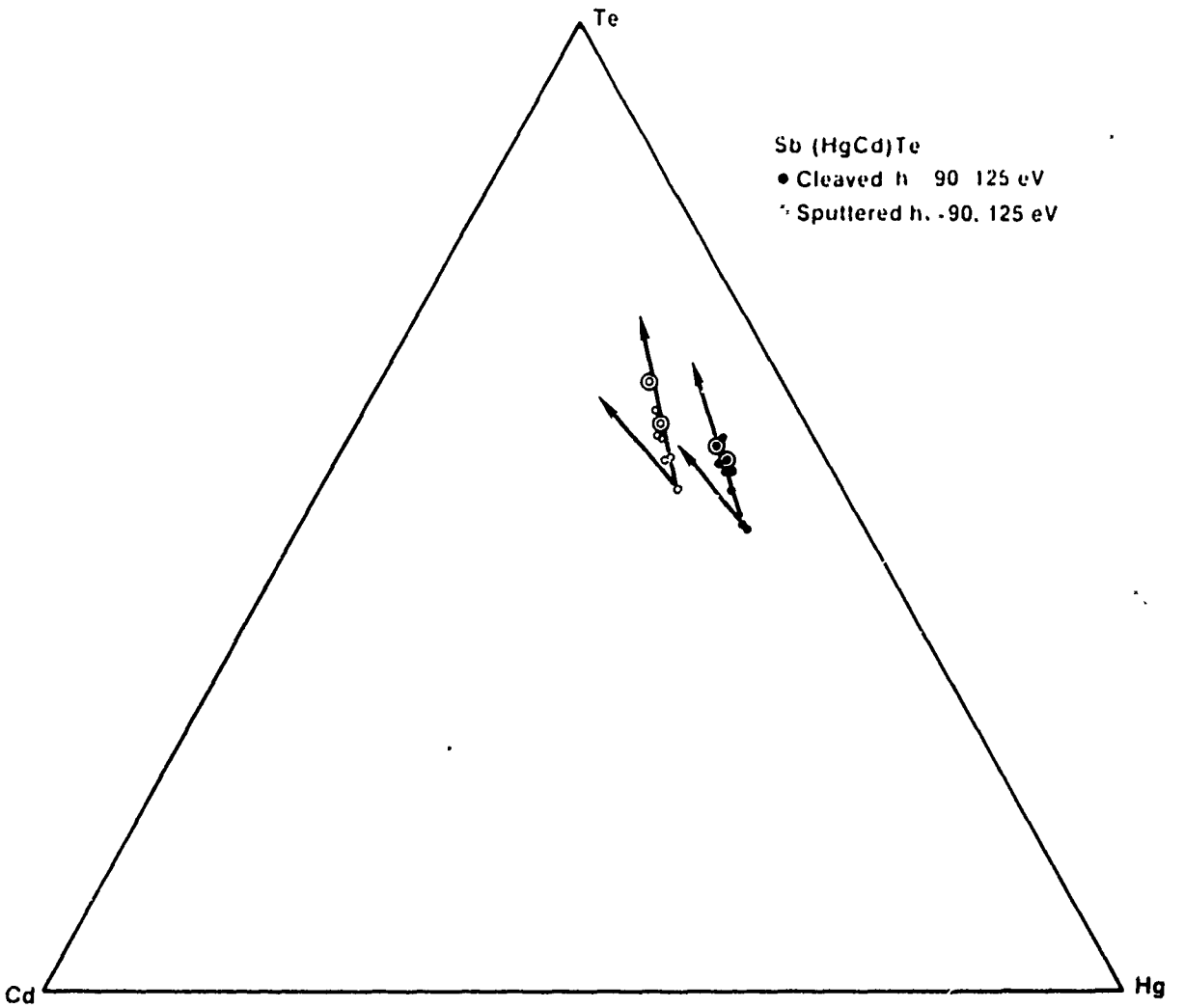

Figure 6: Hg-Cd-Te SBD illustrating the evolution of the semiconductor-component composition during Sb deposition onto both cleaved and sputtered substrates. Points representing the deposition of 10-20 Åcircled.

the Cd and Hg become diluted in the growing overlayer while the Te signal would remain strong. The data suggest that both processes are involved, but their relative importance is unclear.

The Sb-(HgCd)Te interface does not exhibit this alloying effect. Unlike the case with Au, the cation and anion signals from the cleaved substrates are attenuated at approximately the same rate (although there may be some nonuniform film growth occurring). The interface, then, is likely to be more stoichiometric than any other one, either measured or predicted, whereas the overlayer is more pure (i.e., there are less diffusing species). In the case of the sputtered substrates, there is some outdiffusing Te, but less than that observed for Au or any reactive metal. This Te probably originates from the elemental Te produced during ion bombardment and not during the deposition process.

Spectral features shift to 0.2 eV higher kinetic energy (lower binding energy) during Au deposition onto cleaved substrates. This shift is due to movement of the Fermi level caused by indiffusion of Au, which acts as an acceptor in (HgCd)Te. (This Fermi level movement reduces the band bending of the surface region, but is not sufficient to overcome the initial inversion of the p-type substrate.) No such shift is seen for Au deposition onto sputtered substrates or for Sb deposition onto either substrate. The lack of Fermi level movement for sputtered substrates is likely due to the large number of sputter-induced defects, which act as donors and continue to pin the Fermi level. In the case of Sb, it either does not diffuse into the (HgCd)Te or does diffuse but is not electrically active, behavior similar to that of Cr.[20–22]

Based on these findings, the interaction between (HgCd)Te and a typical unreactive overlayer can be described as follows: The substrate surface is inert to the overlayer material, so that the deposited material remains in the elemental state even during the very initial stages and a stoichiometric interface is formed. If elemental Te is present on the surface, as in the case of sputtered (HgCd)Te, the overlayer can react with it to form a small amount of telluride. Other factors, such as heats of cation alloying, may also influence the interfacial behavior.

Intermediate Reactivity Overlayers

Because intermediate reactivity overlayers form tellurides with heats of formation near that of HgTe, the net energetics of exchange reaction 3 are small and the extent of the reaction can be governed by other factors. One such factor that has already been discussed is the heat of cation alloying. Because the Au-HgTe exchange reaction is endothermic and the heats of cation alloying in Au are only moderate, this phenomenon has only a minor effect on the interfacial behavior. In other cases, notably Pt[30] and Pd,[53] the heats of cation alloying can dominate the interfacial reactions.

Other factors that can govern the interfacial behavior for the intermediate reactivity class of overlayers are the stability of the surface and the propensity of the overlayer to diffuse into the semiconductor. We illustrate these effects with Ge[26,27] and Ag,[18,19,26,28] respectively.

The Ge-(HgCd)Te interface exhibits different behavior depending on whether the substrate is cleaved or sputtered. The Hg-Cd-Te SBD of Fig. 7 illustrates this effect. The cleaved surface loses only a little Hg during overlayer growth (as indicated by the semiconductor-constituent composition proceeding directly toward the Te vertex), whereas the sputtered surface loses two to three times as much, relative to Cd[26,27] (as indicated by the composition proceeding in a bowed path between the two model evolutionary lines). Apparently the net energetics of the Ge-HgTe exchange reaction are slightly negative, so that Ge acts as an unreactive overlayer on a cleaved substrate. On the other hand, the ion bombardment induces surface defects, including broken, distorted, and like-like bonds. These defects decrease the stability, or increase the reactivity, of surfaces in general[54] and of (HgCd)Te surfaces in particular.[26,27] Some of these damaged bonds are sufficiently weakened that the exchange reaction can occur and the loss of Hg from the interface is increased. (The formation of a telluride from Te-Te bonds is favorable in all cases, including unreactive overlayers; however, since there is no Hg associated with this reaction, there is no change in the Hg/Cd ratio.) This mechanism is further supported by an increase in the Hg loss from sputtered $Hg_{0.7}Cd_{0.3}Te$ material compared with $Hg_{0.8}Cd_{0.2}Te$ material.[26,27] This enhanced Hg loss is likely caused by an increase in the preferential sputtering of Hg (and consequently, ion bombardment-induced damage)[17] which, in turn, is believed to be caused by the small decrease in stability of the Hg-Te bond due to alloying.[5–7] The difference in behavior of cleaved and sputtered substrates upon deposition of Ge suggests that this interfacial interaction is a sensitive indicator of the stability of the (HgCd)Te

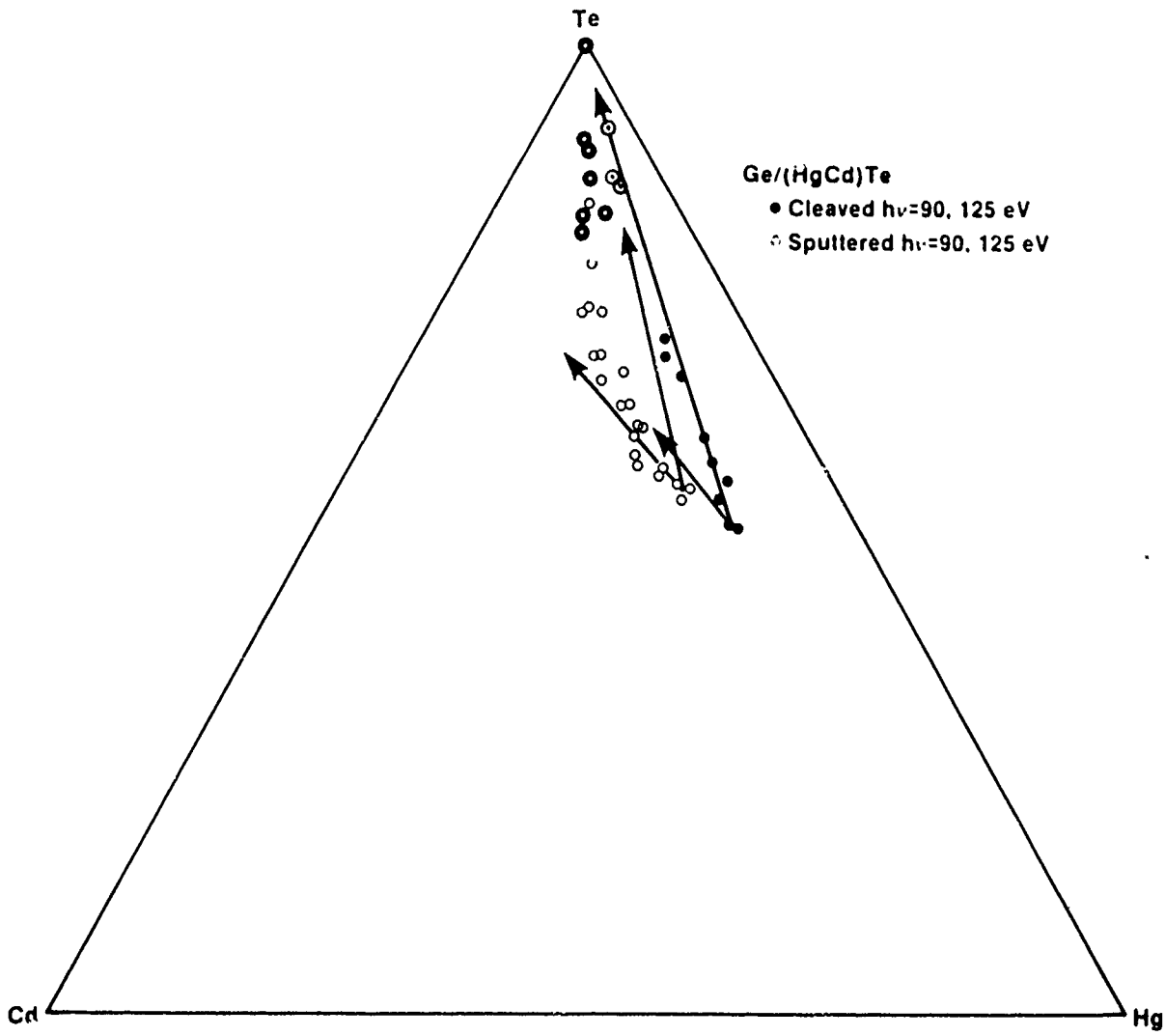

Figure 7: Hg-Cd-Te SBD illustrating the evolution of the semiconductor-component composition during Ge deposition onto both cleaved and sputtered substrates. Points representing the deposition of 10-20 Åcircled.[26]

surface.

Significant variations between the interactions of Ag with cleaved and sputtered substrates are also seen, but are manifested in different ways.[26] In addition, variations are also seen between the results on cleaved surfaces from different groups.[18,19,26,28] The latter differences are clearly seen in the Hg-Cd-Te SBD of Fig. 8. Both Davis et al.[26] and Friedman et al.[18,19,28] report significant indiffusion of Ag during deposition; this is reflected by the nearly constant semiconductor-component composition of the SBD, especially for coverages less than 20 Å, and by the slow rise in the Ag signal from cleaved substrates during overlayer growth (Fig. 9). However, while Friedman et al. report a large loss of Hg from the surface region as indicated by the evolution of their results directly away from the Hg vertex, Davis et al. found no decrease in the Hg (relative to Cd). Two possible explanations for this difference have been advanced:[26] material and surface quality. The two research groups obtain their material from different sources (Cominco and Santa Barbara Research Center, respectively), there may be an inherent material difference that makes one more susceptible to Hg loss. Such a material difference was previously suggested to explain variations in the stability of samples in ultrahigh vacuum.[7] Alternatively, differences in cleavage quality could be responsible for the observed variation. Cleaved (HgCd)Te surfaces are of much poorer quality than Si or GaAs cleaved surfaces.[55] Because Friedman et al. use larger samples, their surfaces may well have more cleavage-induced defects that could enhance a loss of Hg. In either case, the results suggest that Ag deposition is also a sensitive indicator of the reactivity or stability of the (HgCd)Te surface.

This sensitivity is also evidenced by variations in behavior between sputtered and cleaved substrates, although these variations are manifested in a different way.[26] Figure 9 shows that the Ag signal grows approximately five times faster on sputtered substrates than on cleaved substrates, indicating that the indiffusion of Ag is greatly slowed or even virtually stopped. Two mechanisms may contribute to this diffusion reduction. The first is a chemical trapping of Ag at the interface with the formation of Ag_2Te or other Ag-Te complexes following reaction with elemental Te or by HgTe weakened by the ion bombardment. Such a reaction product is supported by a chemical shift of the Ag peak seen only from sputtered substrates. The second possible mechanism, depending on the diffusion processes, would be a disruption of diffusion paths with the formation of an amorphous surface region.

Unlike the other classes of overlayers, the behavior of interfaces formed by inter-

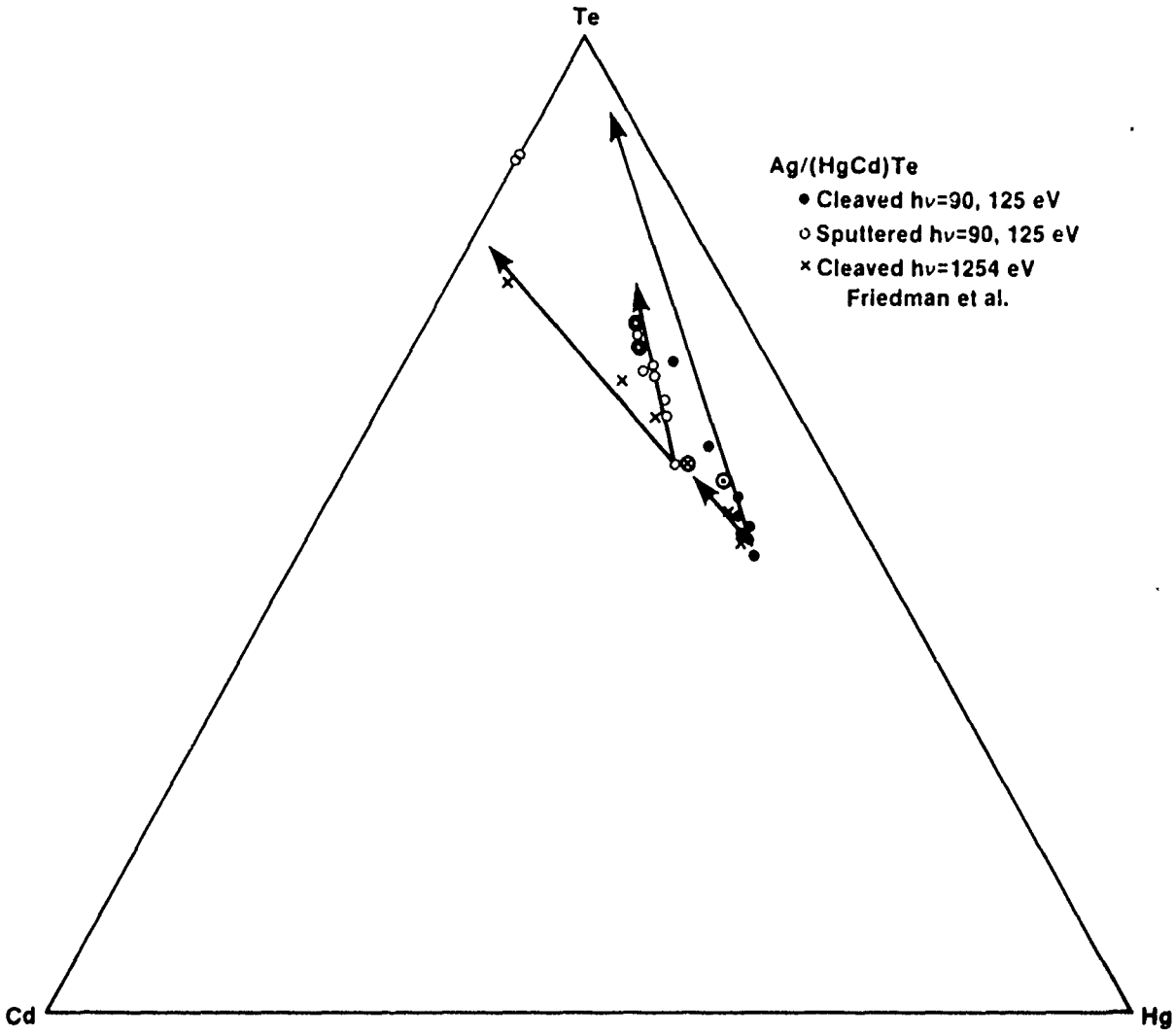

Figure 8: Hg-Cd-Te SBD illustrating the evolution of the semiconductor-component composition during Ag deposition onto the cleaved and sputtered substrates of Davis et al.[26] and the cleaved substrates of Friedman et al.[18] Points representing the deposition of 10-20 Åcircled.[26]

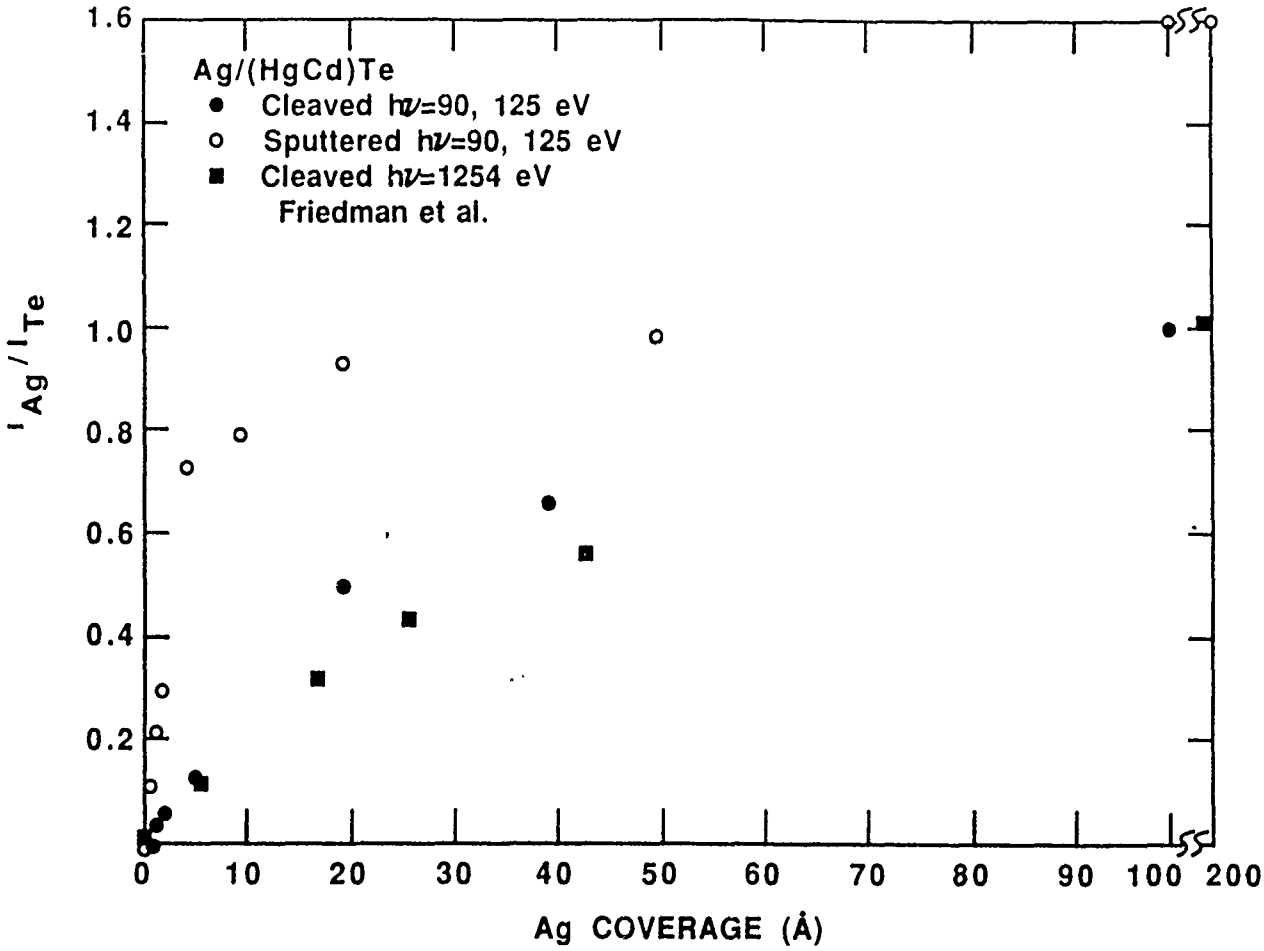

Figure 9: Ag/Te intensity ratio as a function of Ag deposition. Results are shown for the cleaved and sputtered substrates of Davis et al.[26] and the cleaved substrates of Friedman et al.[18]

mediate reactivity overlayers are governed by the heat of formation of their tellurides only in the sense that the HgTe exchange reaction has a near-zero driving force and, hence, the direction in which reaction 3 would proceed can be influenced by other factors. These factors include surface stability and quality, which can make the surface more reactive, as well as heats of cation alloying or propensity of the overlayer element to diffuse into the (HgCd)Te. (The last two factors could also affect the behavior of unreactive metals- (HgCd)Te interfaces.) Because of the ease at which the interaction of these materials with (HgCd)Te is governed by such other factors, they serve as a probe of the surface stability or reactivity.

2. Overlayer/Interlayer Structures

Two families of overlayer/interlayer structures were investigated: Ag/(Sb,Al,Ti)/(HgCd)Te[31] and Sb/(Al,Ti)/(HgCd)Te.[25] The first of these explores the use of a diffusion barrier to block the rapid indiffusion of Ag. We chose interlayers with a wide range of reactivities to examine the role of interlayer chemistry in controlling interfacial behavior. The second of these explores the use of a diffusion facilitator to possibly increase the indiffusion of Sb.

Ag/(Sb,Al,Ti)/(HgCd)Te

The Ag/(Sb,Al,Ti)/(HgCd)Te systems were chosen to examine the effectiveness of different interlayers to control overlayer indiffusion and reaction with the substrate. As we have already seen, Ag diffuses rapidly into (HgCd)Te so that relatively little is accumulated at the surface even after 20 nm of deposition. Additionally, the differing results, especially concerning Hg loss, by different groups suggest that the interfacial interactions are very sensitive to surface stability. As such, this system provides a severe test of potential diffusion barriers and interfacial behavior modification. The interlayers chosen exhibit a wide range of reactivities, with Sb being one of the least reactive of all possible materials and Ti being one of the most reactive. They allow the role of the interlayer chemistry in controlling interfacial behavior to be investigated.

Ag/Sb/(HgCd)Te: The normalized intensities of the semiconductor and interlayer components as a function of overlayer coverage are presented in Fig. 10 for the Ag/Sb/(HgCd)Te system. For comparison, the same quantities without the Sb overlayer are presented in Fig. 11.[26] Figure 10 shows that all three semiconductor constituents are attenuated equally by the Sb interlayer, as expected from its unreactive nature.[11] During Ag deposition, the cation signals continue to decrease steadily, albeit at a rate slower than expected from attenuation length considerations, until the Hg signal is lost in the noise at 5 nm Ag and that of Cd becomes undetectable at 10 nm Ag. Such behavior is very different from that occuring without an interlayer, where all semiconductor signals remain very strong even at 10 nm Ag.

The Te and Sb signals during Ag deposition exhibit different trends. The Te peak intensity increases (compared to its Sb-attenuated value) during low Ag coverages (<1 nm) to a maximum of 70% of its initial value on the cleaved surface and then slowly decreases at higher coverages. On the other hand, the Sb peak has a constant intensity up to 10 nm Ag, suggesting that the Sb floats on top of the Ag layer.

Figure 12 shows the relative rate of increase of Ag for the three different interlayers discussed here and for the case of no interlayer. Initially, the Ag builds up approximately three times faster on the surface with the Sb interlayer than on the control cleaved surface although the amount of detectable Ag on the two surfaces is nearly identical at 10 nm Ag. However, if the Sb layer floats on the Ag surface, the Sb would attenuate the Ag signal and the amount of Ag in the surface region would be 2.5-3 times greater for high coverages as well.

During Ag deposition, the Sb peak broadens due to an unresolved component at 0.5-0.6 eV higher binding energy. This second species is most pronounced in the 0.5-2 nm Ag range, where it is comparable in intensity to the original species. The new component then diminishes in intensity although it remains detectable up to our highest coverages. The Te peak sharpens slightly during Sb deposition and remains sharp for all Ag coverages, reflecting a single chemical species (or two species that exhibit identical binding energies).

During Sb deposition, all spectral features shift 0.2 eV to lower kinetic energy. That is, band bending occurs so that the Fermi level moves into the conduction band as is frequently seen during metals deposition.[10,11] However, this movement is reversed by 0.05-nm Ag deposition as the peaks all return to their initial values and remain there with higher Ag coverages. A similar change in band bending was observed with

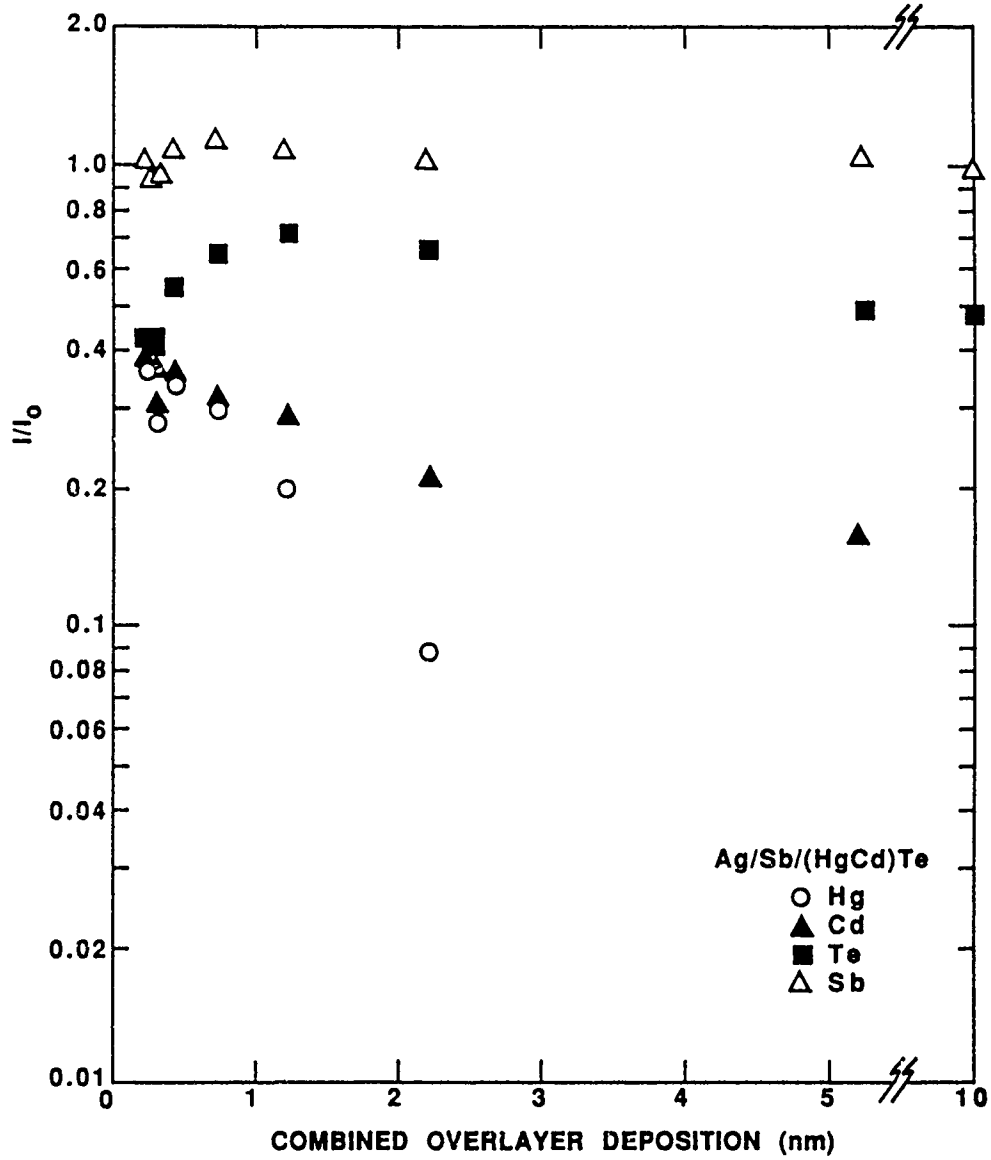

Figure 10: Normalized intensities of Hg, Cd, Te, and Sb as a function of combined overlayer deposition for the Ag/Sb/(HgCd)Te system.

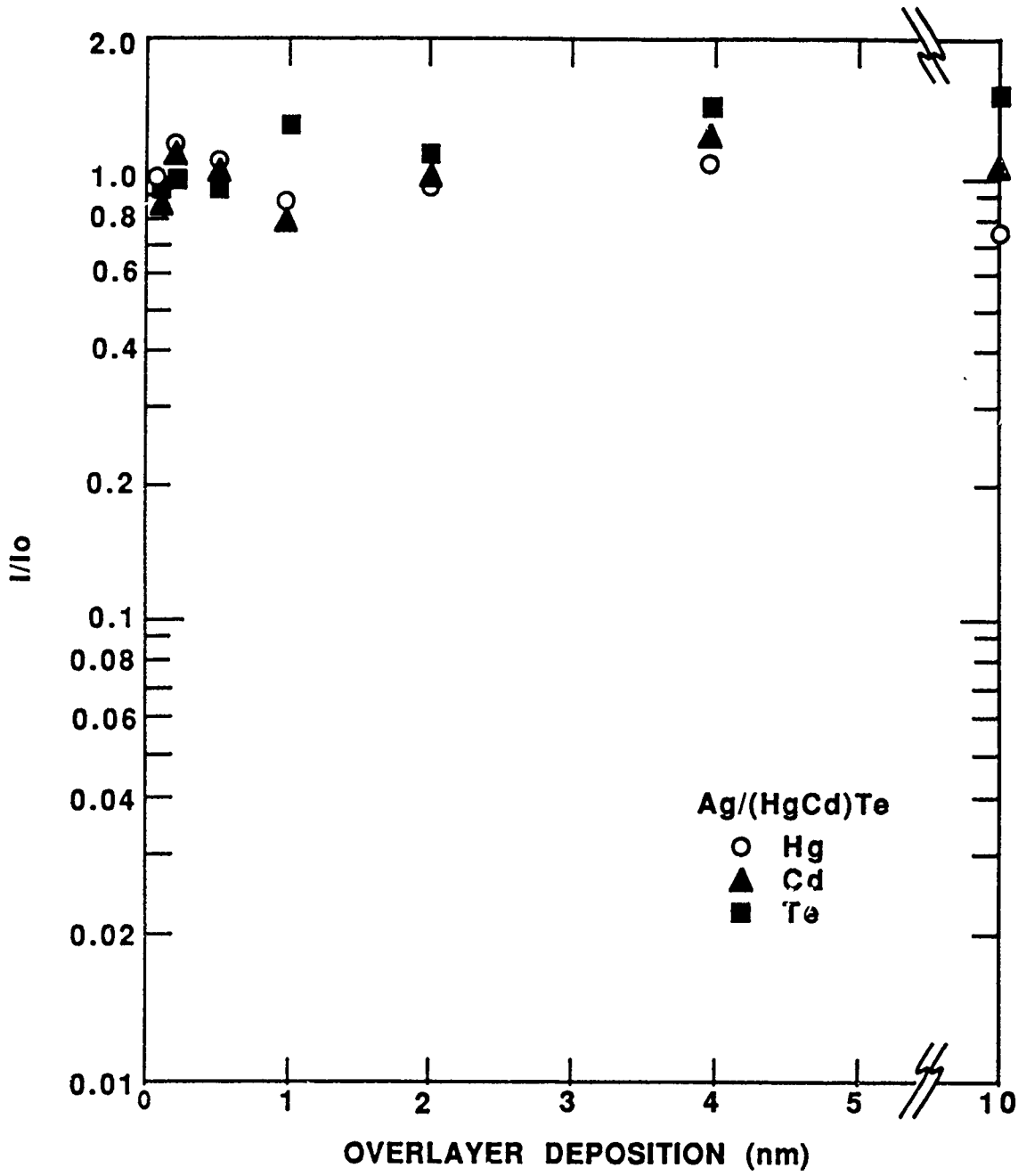

Figure 11: Normalized intensities of Hg, Cd, and Te as a function of Ag deposition for the Ag/(HgCd)Te system. (Adapted from ref. 26 .)

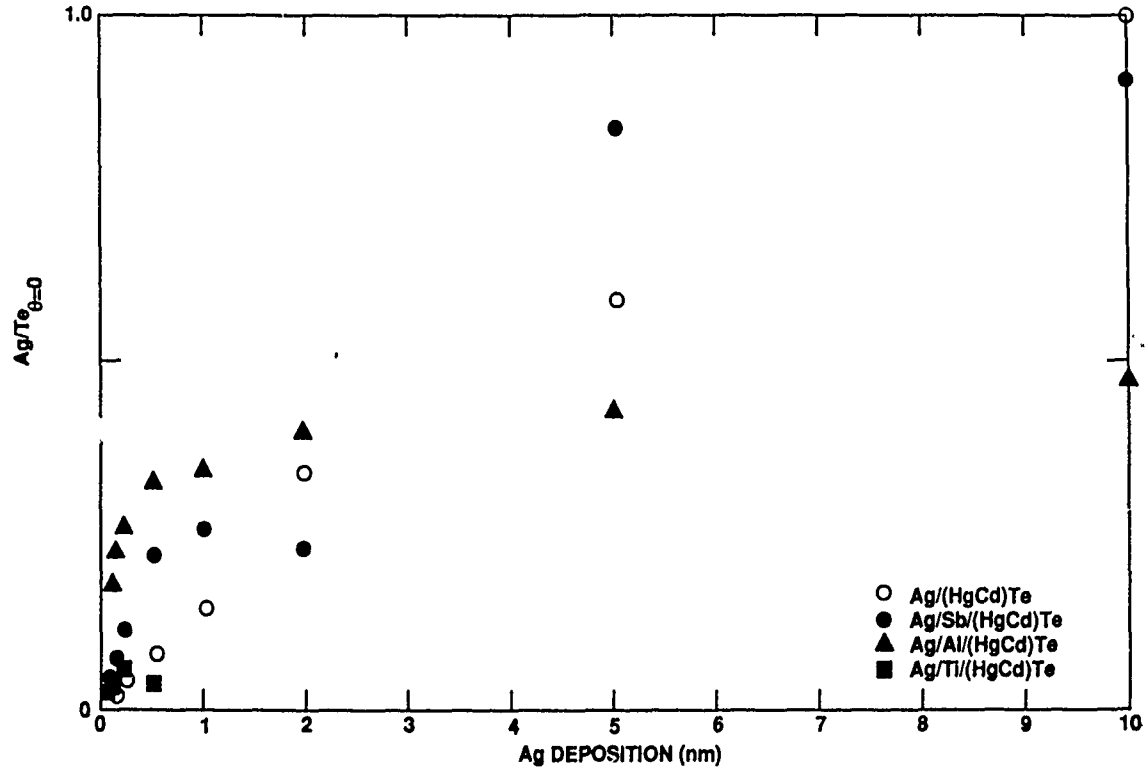

Figure 12: Ag intensity, normalized to the initial Te intensity, as a function of combined overlayer deposition.

Ag deposition without an interlayer.[26]

Ag/Al/(HgCd)Te: The normalized intensities of the different spectral peaks for the Ag/Al/(HgCd)Te system are given in Fig. 13. During the Al deposition, the expected changes occur – the Cd signal is attenuated according to the predicted attenuation length of 0.2 nm; the Hg signal is reduced even more, reflecting a loss of Hg from the interface; and the Te signal increases, reflecting the formation of Al_2Te_3. The semiconductor and interlayer peaks continue to diminish exponentially for the first 0.2-0.5 nm Ag, but except for that of Hg at the highest coverages, remain essentially constant for further depositions.

The Ag signal intensity follows an opposite trend (Fig. 12). It increases very rapidly at first – approximately ten times the rate of increase with no interlayer. However, after 0.5 nm Ag, it only slowly increases, so that at 10 nm Ag, the Ag peak is only half as large as that of the control with no interlayer. In this case, it cannot be argued that the Ag layer on the semiconductor surface (interface) has been attenuated and is greater than it seems, because all semiconductor and interface peaks persist at high coverages.

Unlike the Sb 4d peak, the Al 2p peak is constant in shape throughout the deposition sequence. It is indicative of a single bound state (Al_2Te_3). The Te 4d peak broadens considerably during Al deposition and then slowly sharpens with increasing Ag coverage, but remains broader than its original shape for all coverages.

During the Al deposition, all spectral features shift to 0.4 eV lower kinetic energy reflecting the change in band bending due to Al indiffusion to act as a donor. During the first 0.2-0.5 nm of Ag, the energy shift is reversed and the peaks return to their original energies (0.1 eV) except for Al, which appears 0.1-0.2 eV lower in kinetic energy. This behavior is very similar to that observed in the case of a Sb interlayer except that it occurs more slowly, i.e., additional Ag is required to reverse the band bending.

Ag/Ti/(HgCd)Te Figure 14 gives the normalized intensities of Hg, Cd, Te, and Ti as a function of combined overlayer coverage for the Ag/Ti/(HgCd)Te system. Deposition of Ti results in a depletion of both Hg and Cd from the near surface region while the Te is nearly constant. Upon deposition of Ag, the Hg and Cd signals

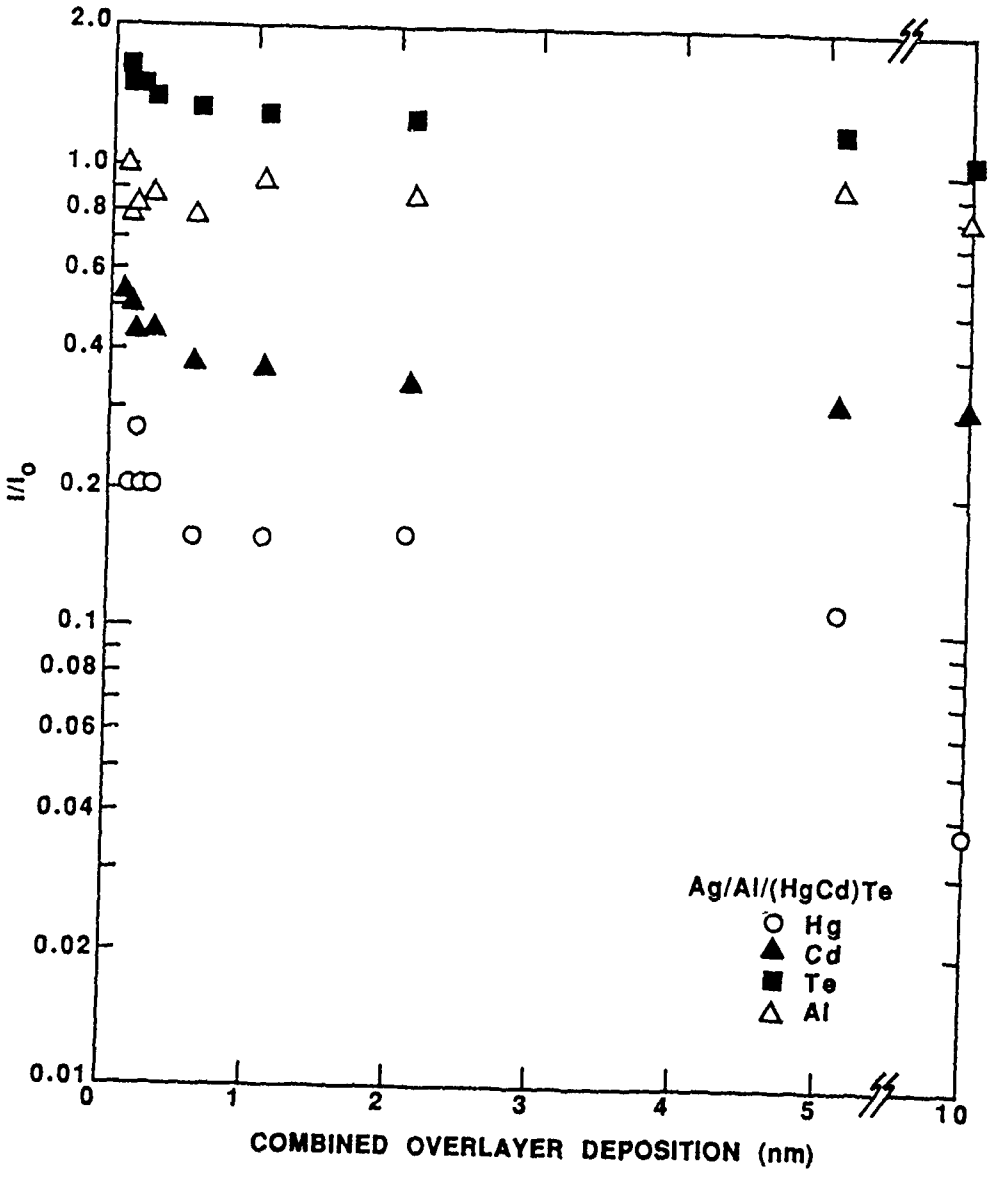

Figure 13: Normalized intensities of Hg, Cd, Te, and Al as a function of combined overlayer deposition for the Ag/Al/(HgCd)Te system.

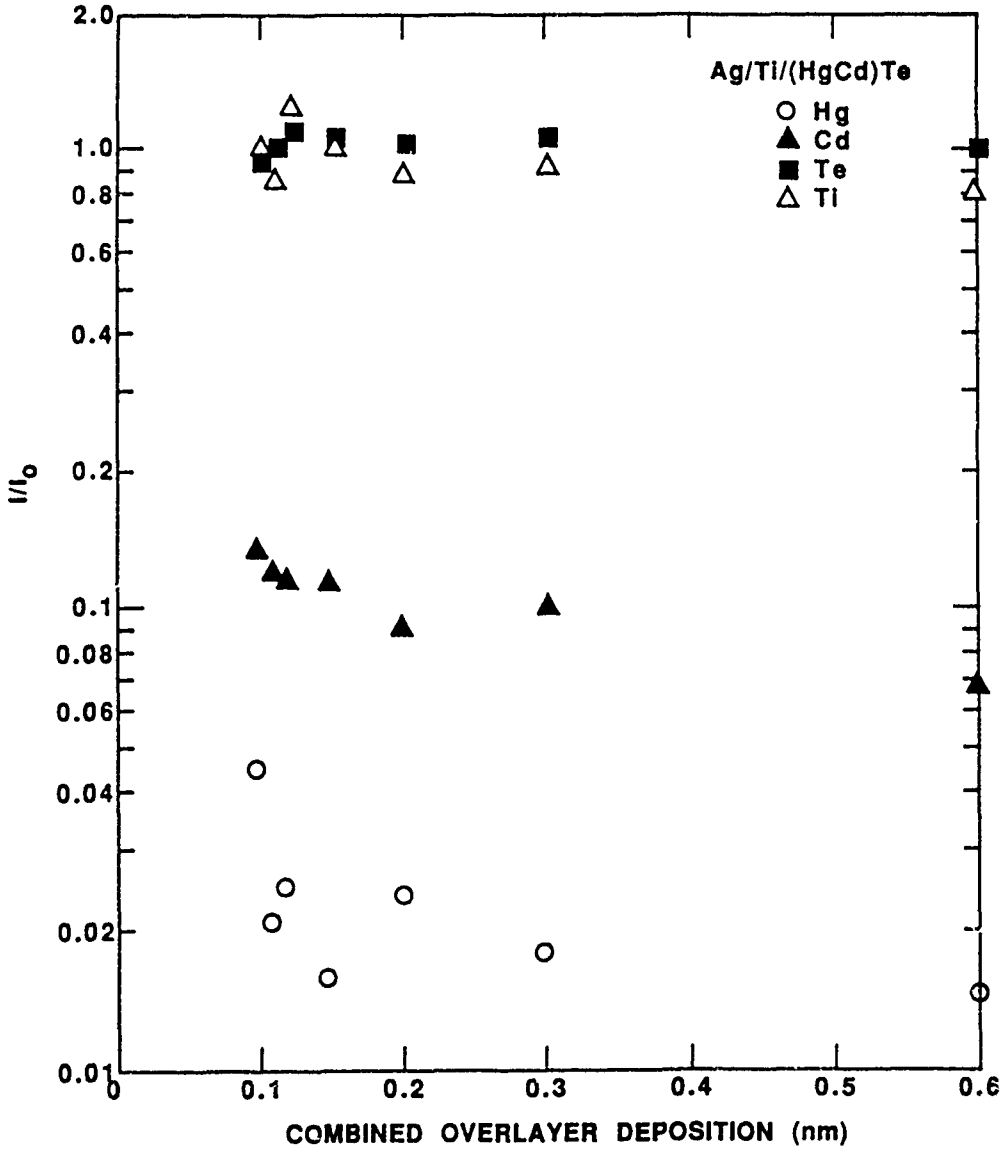

Figure 14: Normalized intensities of Hg, Cd, Te, and Ti as a function of combined overlayer deposition for the Ag/Ti/(HgCd)Te system.

continue to decrease (but only slowly), and both the Te and Ti signal intensities remain unchanged.

In contrast to the behavior observed with the Sb and Al interlayers, the Ag peak grows no faster than it does on a cleaved surface with no interlayer (Fig. 12). Although the coverage data with the Ti interlayer is limited, the Ag intensity after 0.5 nm Ag is less than half of that observed after 0.01 nm Ag for the Al interlayer.

The Te 4d peak broadens during Ti deposition and retains the same shape throughout the abbreviated Ag deposition sequence – a behavior much like that observed during similar Ag coverages following Al deposition. The Ti 3p peak is also broad and maintains the same shape.

During neither Ti or Ag deposition is there a discernable change in the band bending. With the exception of the Te peak which shifts by $\approx$0.2 eV to higher kinetic energy with Ag deposition, the spectral features appear at fixed energies.

Discussion: The data presented above indicate that thin (monolayer) interlayers can significantly alter the interfacial behavior observed following Ag deposition onto (HgCd)Te. The greatest difference is noted with an Sb interlayer. This interlayer is inert and forms an abrupt, stoichiometric interface with the (HgCd)Te. This elemental Sb layer partially "passivates" the surface so that the cation signals are eventually reduced to below our detectability limit and the Ag accumulates in the surface region approximately three times faster than with the control. Nonetheless, it is likely that some Ag continues to diffuse into the substrate because of the slow attenuation of the Cd peak and the moderate Ag accumulation rate (which is approximately three times slower than that observed initially with the Al interlayer).

Although the effects of even thinner interlayers can be substantial in many cases,[1] the changes induced in the behavior of the Ag/(HgCd)Te system by the Sb interlayer, in particular, are surprising considering that the interlayer floats on top of the Ag. We speculate that the Sb partially heals and/or clogs the defects that allow the rapid indiffusion of Ag.[26] In this case, only a small, undetectable fraction of the Sb would be required to remain at the interface. Additionally, there may be a synergistic effect between the Ag and Sb that allows some interaction with the HgTe component. Such a reaction would explain 1) the increased attenuation of the Hg signal compared to that of Cd, 2) the persistance of the Te, and 3) if there were the formation of an Ag-

Sb-Te complex, the broadening of the Sb peak that coincides with the maximum in the Te intensity curve. A Ag complex would also help to trap Ag in the surface region and reduce indiffusion. A synergistic effect is also consistent with the differences in published results for the Al/(HgCd)Te system (see above). Because the net energetics of the Ag-HgTe exchange reaction are small, small changes in surface stability would be sufficient to alter the direction of the reaction. In this case, the presence of the Sb would allow the exchange reaction to proceed, at least partially.

In the case of an Al interlayer, all substrate peaks are detectable even at the highest coverages (10 nm Ag). For the first few tenths of a nanometer of Ag, the substrate and interlayer peaks decrease and the Ag peak rapidly increases, indicating that Ag is accumulating at the surface and that little is diffusing inward. However, the situation is much different at higher coverages. There, the rate of accumulation of Ag decreases and attenuation of other signals slows dramatically, if not stopping completely, and indiffusion of Ag occurs as if the interlayer was not present.

The Ti interlayer is the least effective in affecting the behavior of the Ag/(HgCd)Te interface. Although the coverage sequence is less extensive, little, if any, attenuation of the substrate and interlayer signals occurs during Ag deposition and Ag accumulates in the surface region at the same rate that it does without an interlayer.

The results for Al and Ti interlayers are quite different from those reported for the Al/Yb/(HgCd)Te system,[56] which also consists of an interlayer more reactive than the overlayer. Raisanen et al. found that Yb forms a diffusion barrier and passivates the (HgCd)Te surface with respect to Al; there is no Al-HgTe reaction and additional Hg is not depleted from the interface. However, there are two important differences between the two sets of experiments. They used a considerably thicker interlayer (1.5 nm or 5 monolayers), which would form a more effective barrier. Additionally Al is more reactive than Ag and tends to be trapped at the interface; it does not diffuse into the substrate except in trace amounts.

In the case of the Al interlayer, the thin Al_2Te_3 layer traps the first monolayer or so of the Ag at the surface, but does not hinder the indiffusion of subsequent Ag. The Ti interlayer also allows the indiffusion to proceed, but from the very beginning. These (ultra)reactive interlayers disrupt the (HgCd)Te surface by reacting with the HgTe and, in the case of Ti, with the CdTe. The resulting tellurides are not sufficiently thick to passivate the surface with regard to indiffusion. In fact, the Al_2Te_3 may even enhance the indiffusion since less Ag is present at the surface following the highest

coverages than is present on the control surface.

For each interlayer, during the initial stages of Ag deposition, the band bending induced during interlayer deposition is reversed (or in the Ti case, no change is followed by no change) so that the relative position of the Fermi level is the same as for the cleaved surface. It therefore appears that the indiffused Ag is able to compensate for electrically active interlayer atoms that diffuse into the substrate, but not for damage induced by cleaving.

Sb/(Al,Ti)/(HgCd)Te

The Sb/(Al,Ti)/(HgCd)Te system was chosen for reasons almost directly opposite those of the Ag/(Sb,Al,Ti)/(HgCd)Te system. Here Sb alone forms a stoichiometric interface with almost no outdiffusion of Te. Additionally, any change in the band bending during Sb deposition is negligible; the sample maintains the same inversion it obtained during the cleaving process. As a result, this system is ideal to investigate whether or not interlayers can increase interfacial reactivity and indiffusion. Two Al interlayers thicknesses were chosen to correspond to the Al_2Te_3 and metallic Al stages (see above); Ti was chosen because it completely disrupts the (HgCd)Te surface and might be expected to cause the greatest change with an Sb interface.

Sb/Al/(Hg,Cd)Te: The normalized intensities in the case of a 0.1-nm Al interlayer are shown in Figure 15. During Al deposition, the Hg becomes depleted from the surface region and Te becomes enhanced. Initially the Hg, Cd, Te, and Al signals fall rapidly upon Sb deposition. However, after 0.05-0.1 nm Sb, the semiconductor and interlayer peak intensities decrease much more slowly, probably the result of clustering or island formation. At the highest Sb converage (5 nm), the Te and Ag peaks are barely detectable while those of Hg and Cd cannot be seen.

Throughout the deposition sequence, the Al peak corresponds to a single, electropositive chemical state, Al_2Te_3. The Te peak broadens with Al deposition, reflecting the presence of both (HgCd)Te and Al_2Te_3 in the detection volume of the measurement. At the highest coverages ($\geq$2 nm Sb), the peak sharpens as the (HgCd)Te component comprises a smaller fraction.

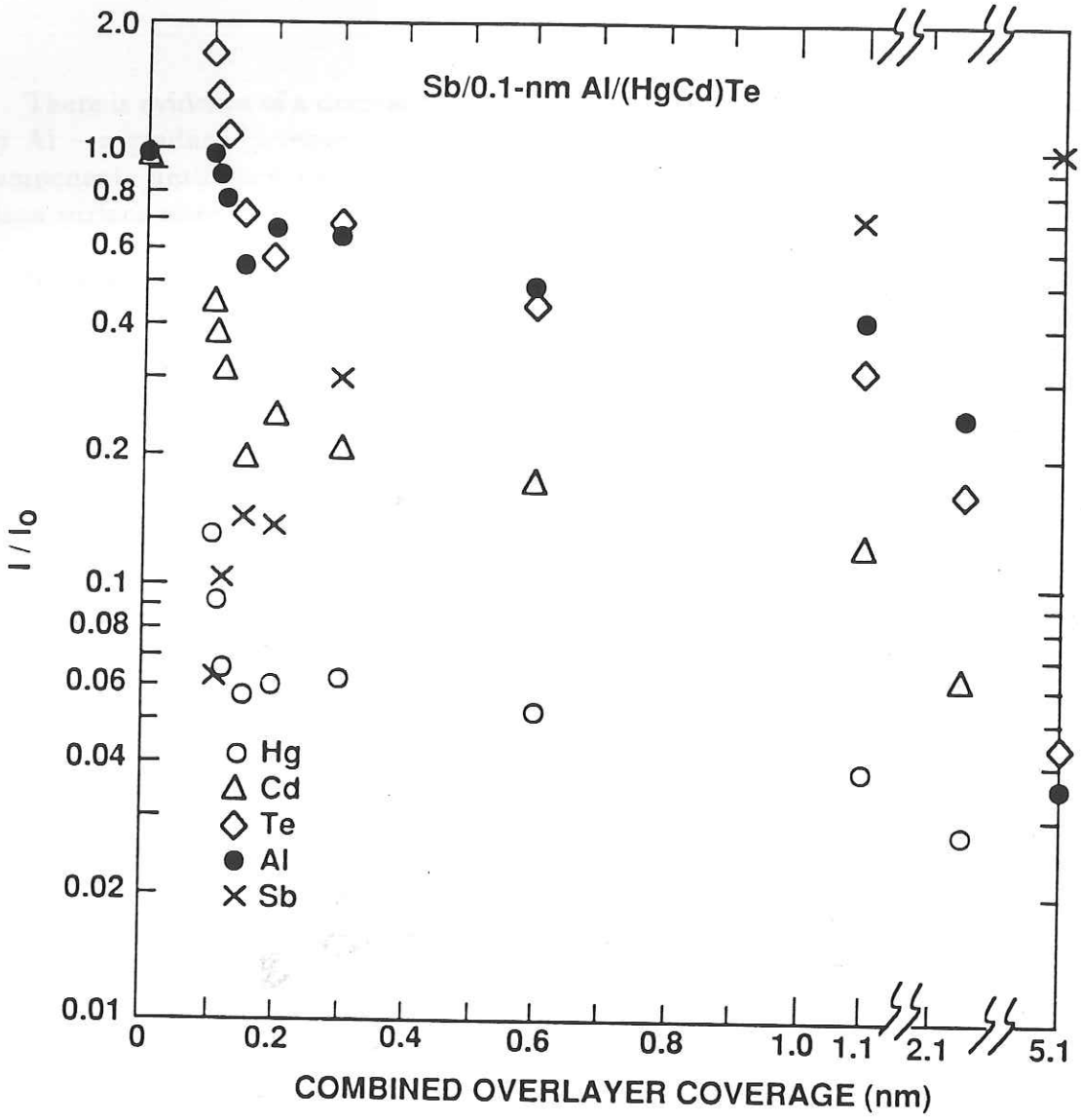

Figure 15: Normalized intensities as a function of combined overlayer thickness for the Sb/0.1-nm Al/(HgCd)Te system. The Hg, Cd, and Te signals have been normalized to the clean surface, the Al signal to the interlayer-covered surface, and the Sb signal to the highest coverage.

There is evidence of a decrease in the additional band bending (0.2-0.3 eV) caused by Al – a gradual increase in peak kinetic energies for each of the semiconductor components until they are within 0.1 eV of their original positions for the cleaved, clean surface after 0.2 nm Sb.

Increasing the Al interlayer thickness has some dramatic effects on the behavior of the Sb/Al/(HgCd)Te system. Following 0.5 nm Al deposition, the Cd signal is only 10% of its original value and the Hg signal is not detectable (Fig. 16). On the other hand, the Te signal is greater than it was initially. The Al peak is dominated by a metallic component with a smaller contribution from Al_2Te_3. As with the thinner Al interlayer, upon Sb deposition, the Cd, Te, and Al signals all decrease according to laminar-overlayer attenuation at first and then only slowly decrease as the Sb clusters.

For each Al interlayer, the total normalized Al signal intensity is reduced at the same rate in both stages (Fig. 17). However, during overlayer growth on the 0.5-nm interlayer, a new component of the Al peak grows at the expense of the metallic one. This more tightly bound component represents AlSb[57]; it is first detectable after 0.02 nm Sb and increases to a maximum at 1 nm Sb before becoming attenuated. Corresponding to this AlSb component, the Sb peak is less tightly bound compared to that associated with the 0.1 nm Al interlayer.

Again, deposition of Sb reverses the increased band bending caused by interlayer growth, but not the inversion induced by cleaving. By 0.05 nm Sb, the kinetic energies of the Te and Cd peaks are within 0.1 eV of their values before Al deposition.

Sb/Ti/(HgCd)Te: In some respects, a 0.02 nm Ti interlayer has a greater effect on the Sb/(HgCd)Te interface than the much thicker Al interlayers in that Ti itself depletes both Hg and Cd from the interfacial region. During Sb overlayer growth, the ratio of Hg and Cd remains constant; although the two cation signals initially are attenuated at the same rate as those with the Al interlayers, they remain detectable even at 5 nm Sb, whereas in the other cases, they do not (Figs. 18 and 19). The difference in behavior of the Te signal is even more pronounced (Figs. 18 and 20). At first, the Te intensity is not reduced at all from its elevated value following Ti deposition. It then is only slowly attenuated and remains easily detectable even after 10 nm Sb; over the range 1-5 nm Sb, it is approximately four times stronger than the corresponding signal in the other two cases.

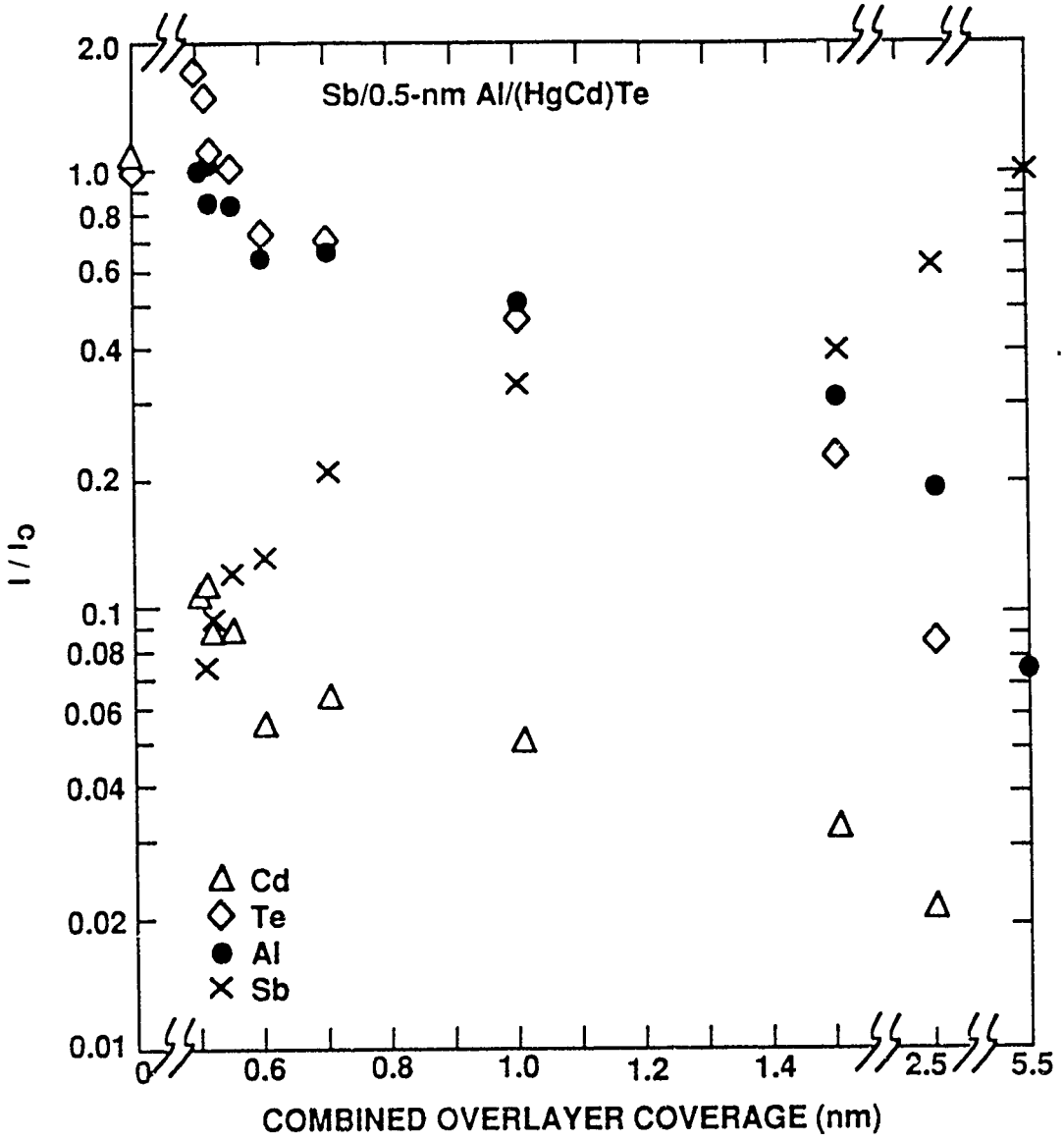

Figure 16: Normalized intensities as a function of combined overlayer thickness for the Sb/0.5-nm Al/(HgCd)Te system. The Hg, Cd, and Te signals have been normalized to the clean surface, the Al signal to the interlayer-covered surface, and the Sb signal to the highest coverage.

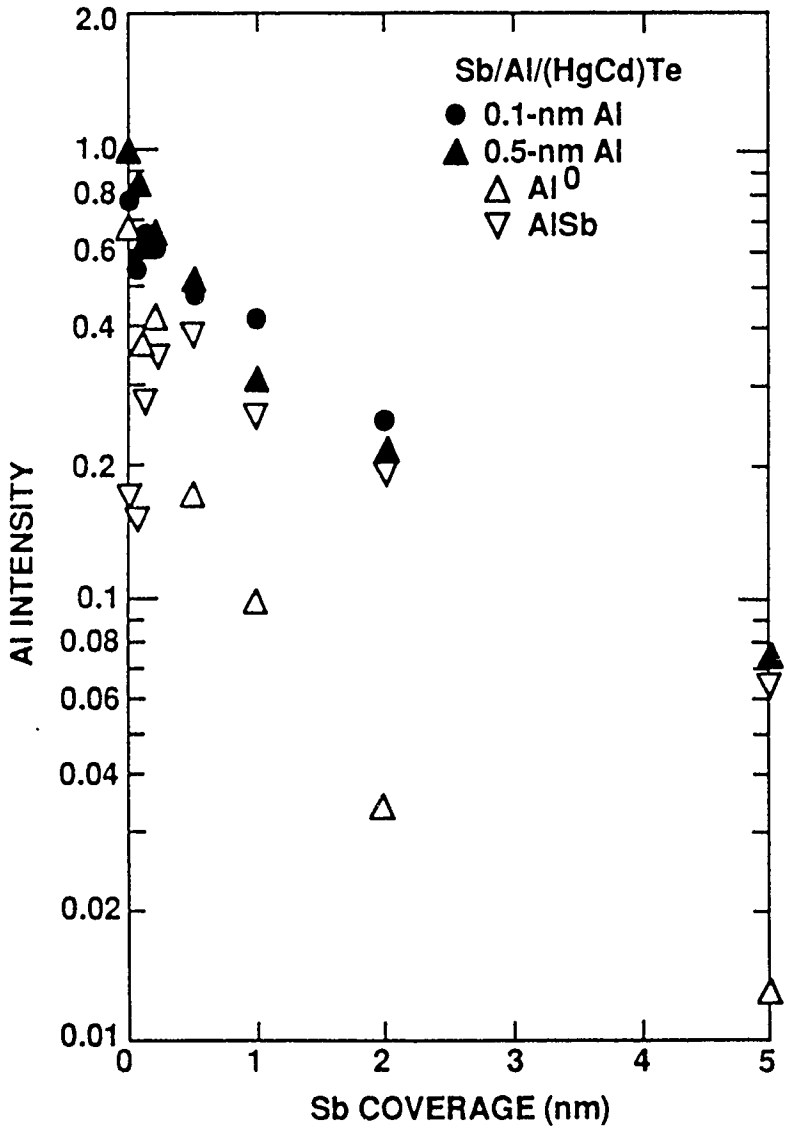

Figure 17: Al intensity as a function of Sb overlayer thickness for the 0.1-nm and 0.5-nm Al interlayers, normalized to the interlayer-covered surface.

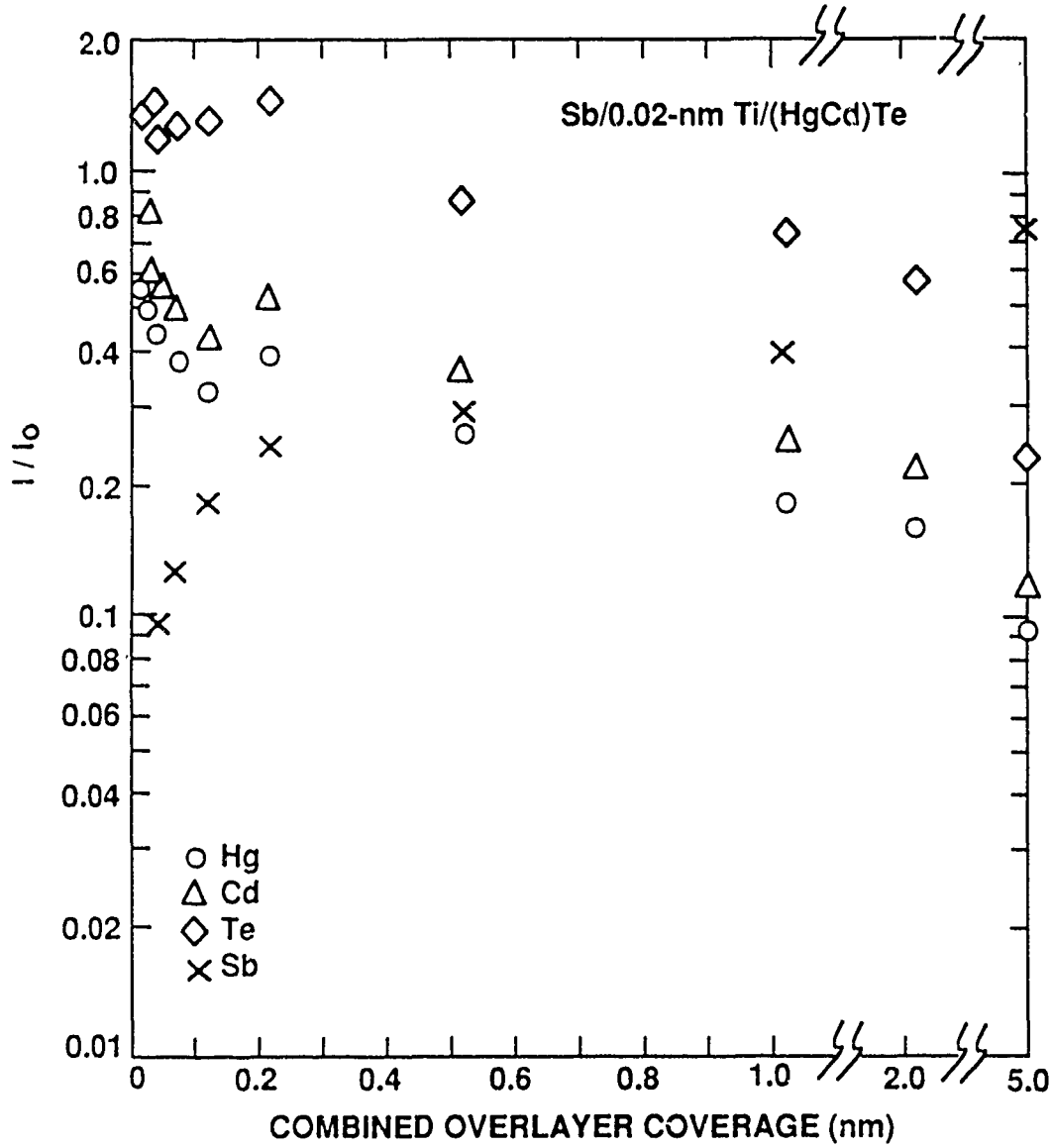

Figure 18: Normalized intensities as a function of combined overlayer thickness for the Sb/0.02-nm Ti/(HgCd)Te system. Normalization is to the clean surface for the Hg, Cd, and Te signals and to the highest coverage for the Sb signal.

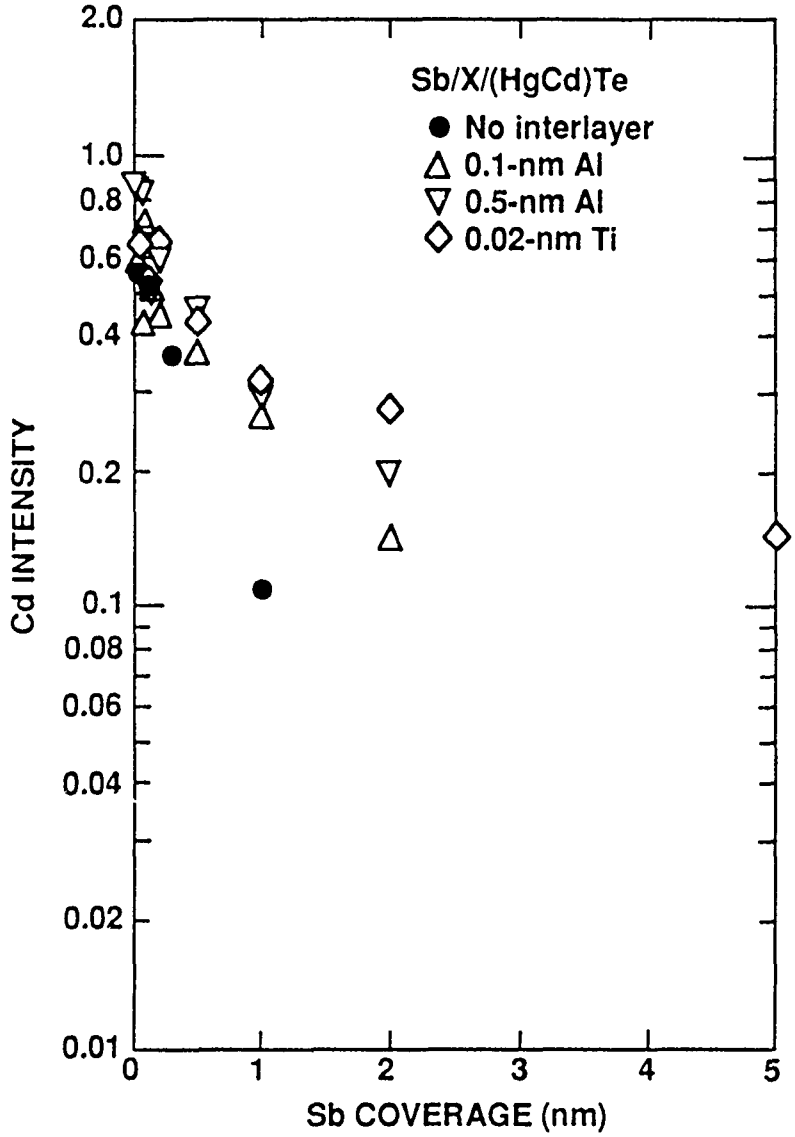

Figure 19: Cd intensity as a function of Sb coverage for the three interlayers and for no interlayer. Normalization is to the clean surface.

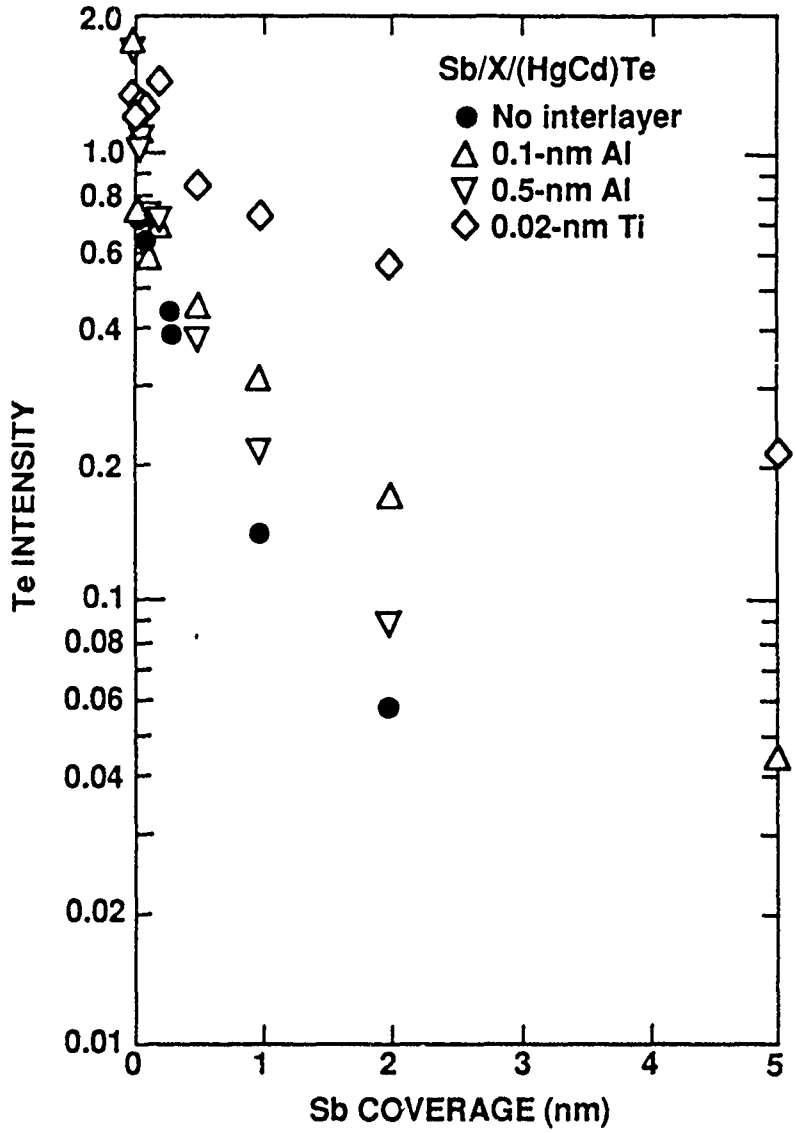

Figure 20: Te intensity as a function of Sb coverage for the three interlayers and for no interlayer. Normalization is to the clean surface.

In another difference between Ti and Al interlayers, deposition of Sb onto the Ti interlayer, reverses the band bending induced by cleavage. (Unlike deposition of Al, deposition of Ti does not cause additional inversion.) The kinetic energies of all spectral features gradually increase throughout the deposition sequence until they are 0.2-0.3 eV greater than their initial values.

Discussion: Thin Al and Ti interlayers alter the behavior of the Sb/(HgCd)Te interface, in some cases substantially. The deposited Sb does not react with either the (HgCd)Te or the interfacial telluride (Al_2Te_3 or Ti_xTe_y), but it does react with the metallic Al that grows after the initial Al has "passivated" the surface with Al_2Te_3. Such a reaction would be expected with any metallic overlayer with which Sb forms a stable compound.

Another change in the growth of the Sb overlayer is the clustering or island growth of Sb. With no interlayer, Sb appears to grow uniformly as indicated by the rapid attenuation of all semiconductor signals. However, with an interlayer, the semiconductor and interlayer signals decrease quickly initially, but remain detectable at relatively high coverages, a behavior typical of many of the overlayers investigated on (HgCd)Te. The clustering is also evidenced by the slower increase in the Sb signal in the range 0.3-50 nm Sb (Fig. 21). This effect is most pronounced for the Ti interlayer where all the semiconductor signals remain detectable up to 5 nm Sb. The alternative explanation of substantial indiffusion, which was observed for Ag, is not likely in this case because of the initial rapid increase in the Sb signal and the similarity in the rise of the Sb signal for all cases, including that of the 0.5-nm Al interlayer, where the formation of AlSb would trap the Sb.

Nonetheless, some indiffusion of Sb is likely and appears to be enhanced by the interlayers. With no interlayer, no change in the inversion that occurs during cleavage is seen, suggesting that Sb does not diffuse or, at least, that any that does diffuse is not electrically active. A few other overlayers, such as Cr[20,22] and Ti,[12] exhibit a similar lack of Fermi level movement, but most induce a change, usually an increase, in band bending. In the case of the Al interlayers, the Al causes additional inversion of the p-type material, but the Sb compensates the indiffused Al and returns the Fermi level to near the conduction band minimum, the nearly universal position for a cleaved surface. The Sb is not able to reverse this initial inversion. The situation for the Ti interlayer is much different. First, the Ti causes no additional band bending,

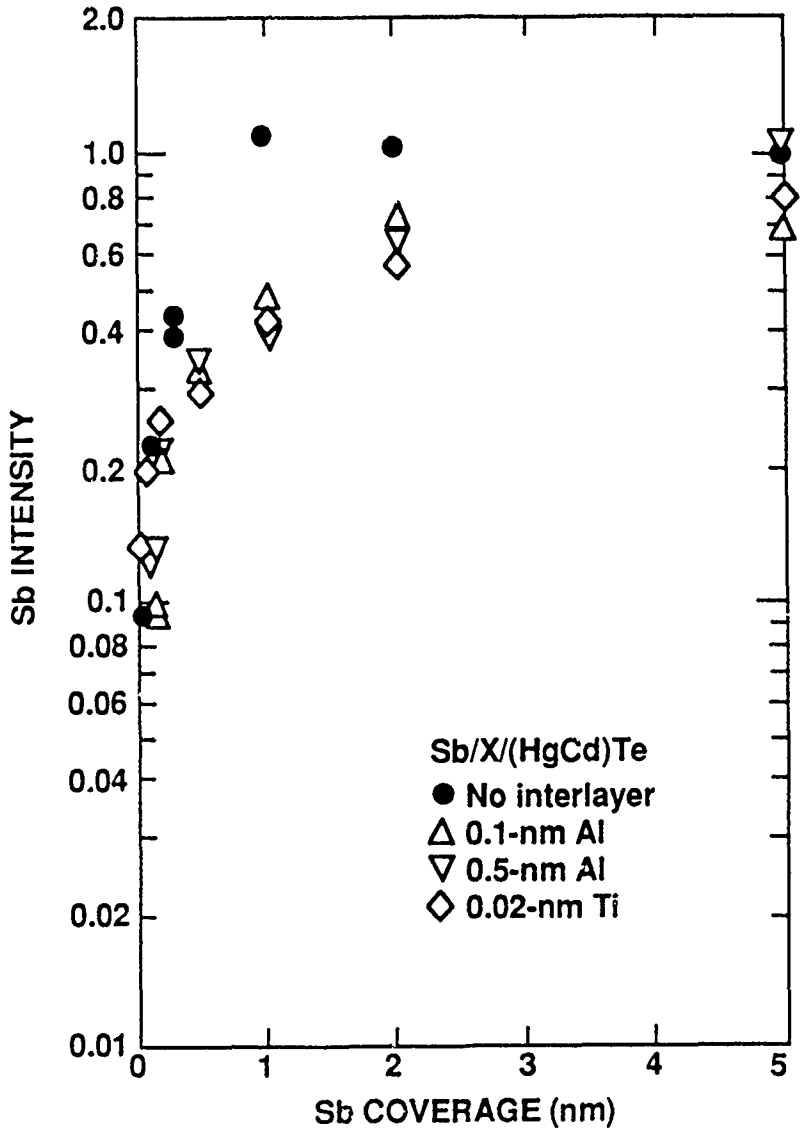

Figure 21: Sb intensity as a function of Sb coverage for the three interlayers and for no interlayer. Normalization is to the highest coverage with no interlayer.

and second, the Sb is able to compensate for the cleavage-induced defects that invert the surface region. Although a small decrease in this initial inversion was observed for Au overlayers,[23] this is the first time that the band bending has been reduced by 0.2-0.3 eV. We propose that this is accomplished by the Ti completely disrupting the (HgCd)Te surface and increasing the Sb indiffusion. Because Ti reacts with both the HgTe and CdTe components, at least at low coverages, it does not tend to passivate the surface with a telluride, but rather promotes greater reaction as seen by the increased loss of Hg from the interfacial region.[12] A similar increase in the indiffusion of an overlayer was possibly seen for Ag[31] despite its rapid indiffusion without the interlayer.

The increased disruption of the (HgCd)Te surface by Ti also leads to enhanced outdiffusion of Te, as evidenced by the slower attenuation of the Te signal compared with that of Cd (Figs. 19 and 20). As a result, the Ti interlayer negates one of the properties of the Sb/(HgCd)Te system that distinguishes it from other (HgCd)Te systems – its abrupt, stoichiometric interface.

The increased interfacial reactivity, at least in the physical sense, with the use of (ultra)reactive interlayers is in marked contrast to the behavior observed by Franciosi and coworkers[56,58] in the Al/Yb/(HgCd)Te system as discussed earlier. However, as before, important differences between the two experiments lead to the different results. These differences include the thickness of the interlayer, heats of solution of Hg and Cd with the interlayer (the cations have high heats of solution in Yb, but endothermic heats of solution in Al[13]), and the reactivity between the interlayer and overlayer (Al and Sb form a covalent compound whereas Al and Yb form an intermetallic compound[59]). In general, thick interlayers are more capable acting as diffusion barriers or passivants. In addition, the high Hg solution enthalpy of Yb causes a two-stage layer growth that further hinders Te outdiffusion and stabilizes the (HgCd)Te surface with respect to Al and other overlayers. These properties are not found in our Al and Ti interlayers; consequently the behavior of the two systems are very different.

III. ELECTRICAL MEASUREMENTS

A. EXPERIMENTAL PROCEDURE

The measurements were performed on contacts to bulk wafers of $Hg_{0.79}Cd_{0.21}Te$ (Au and Al) and $Hg_{0.7}Cd_{0.3}Te$ (Ge) obtained from Cominco American. At 77K (295K), the $Hg_{0.79}Cd_{0.21}Te$ was p-type (n-type) with a carrier density of $2.4\times10^{16}cm^{-3}$ ($1.4\times10^{16}cm^{-3}$) and mobility of 580 $cm^2/V-s$ ($7.7\times10^3cm^2/V-s$). At 77K (295K) the $Hg_{0.7}Cd_{0.3}Te$ wafer was p-type (n-type) with a carrier density of $7.4\times10^{15}cm^{-3}$ ($2.4\times10^{15}cm^{-3}$) and a mobility of 450 $cm^2/V-s$ ($2.6\times10^3cm^2/V-s$). The contact deposition procedure was designed so that the deposition of the first 100 Å would simulate as closely as possible the depositions used for previous chemical measurements.[60] Deposition took place in a stainless steel ultrahigh vacuum chamber operating at a base pressure of about 10^{-9} Torr. Just prior to deposition, the samples were bombarded with 1.5 keV argon ions for five minutes, and then 100 Å of the contact metal was deposited from a tungsten filament at a deposition rate of about 1 Å/sec, as monitored by a quartz crystal located near the sample. The sample was transferred to a diffusion-pumped high vacuum chamber where an additional 1000 Å of the contact metal was deposited. This procedure was chosen because it can also be used (without the ion sputtering) on vacuum-cleaved surfaces.

The contact pattern is shown in Fig. 22. Circular contact pads with diameters of 10, 30, 100, and 300 μmwere defined by covering the contact pad areas with photoresist and then ion milling to remove the uncovered metal. To facilitate attachment of wires to the pads a layer of polyimide was spun onto the wafer and small holes (smaller than the contact pads) were opened through the polyimide down to the contact pads. Gold bonding pads were then evaporated and delineated using the liftoff technique. The sample was mounted in a leadless chip carrier (LCC) and 1-mil-diameter gold

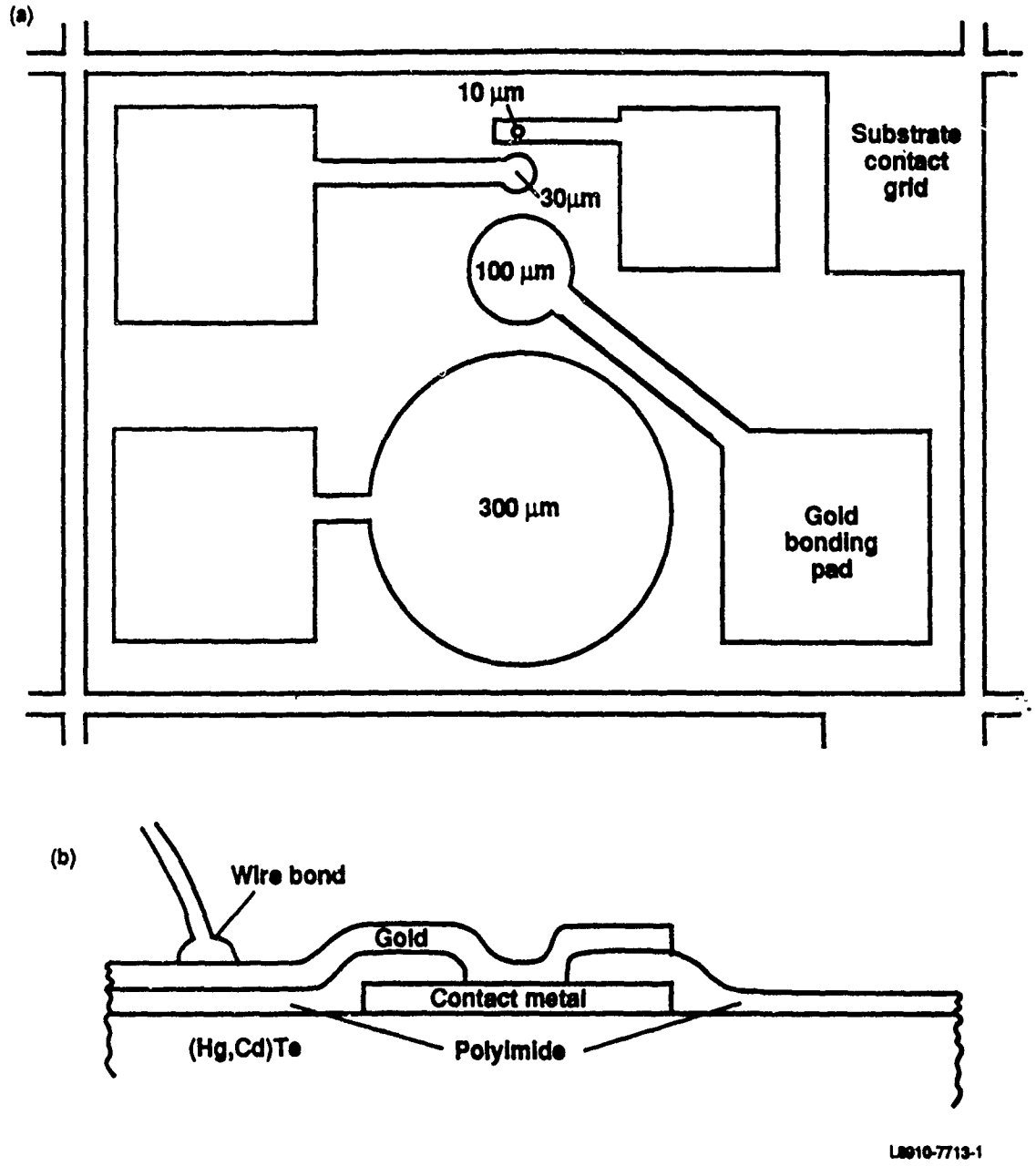

Figure 22: a) Layout of contact pads and substrate contact grid. b) Cross-section of contact pads.

wires were attached with either gold epoxy or thermocompression bonding.

The sample (in its LCC) was mounted in a Hansen liquid helium gas-flow cryostat for electrical characterization. The current-voltage (I-V) characteristics were measured between a contact pad and the large ohmic contact grid. Because of the large size of the grid, the I-V characteristic was limited by, and representative of, the contact pad. The contact resistance was measured between the contact pads and the ohmic contact grid. The intent was to use the Cox and Strack analysis[61] to deduce the contact resistivity from the functional dependence of the resistance on the contact diameter.

The contact noise from a pair of contacts (with equal diameters) was determined using the bridge circuit shown in Fig. 23, which is similar to the arrangement used by Scofield[62] to measure 1/f noise in thin metal films. When the bridge circuit is balanced by adjusting the precision wire-wound decade resistors, R_1 and R_2, correlated signals that are common to both halves of the bridge (e.g., temperature drifts, electromagnetic pickup, or noise in the substrate contact R_{sub}) are cancelled. On the other hand, the noise in the two contact pads, R_{c1} and R_{c2}, and in the substrate material connecting the contacts to the substrate contact grid, R_{s1} and R_{s2}, are uncorrelated, so that the output contains the sum of the noise power from the contacts (and connecting substrate). Therefore, the low-frequency contact noise can be separated from other low-frequency components that are common to both halves of the circuit.

To avoid low-frequency preamplifier noise, an ac technique[62,63] was used. A 1-kHz ac carrier current was driven through the bridge, so that the resistance fluctuations in the contacts appeared as noise sidebands on the carrier. The output of the bridge was fed to a transformer-coupled (100:1) PAR 116 preamp plugged into a PAR 124A lock-in amplifier. The lock-in amplifier demodulated the carrier to retrieve the low-frequency noise signal. The output of the lock-in amplifier was then fed to an HP 3562 low-frequency spectrum analyzer.

A vacuum cleaver was installed on the UHV deposition system so that we could fabricate contacts to vacuum-cleaved material. Extra-thick (2 mm) wafers were obtained so that there would be room on the end of the cleaved wafer to form the contact test pattern (Fig. 22). Two samples, consisting of Au contacts to the vacuum-cleaved wafers, were deposited. These wafers were processed in special wafer carriers that positioned the cleaved (and metal coated) end of the wafer flush with the surface of

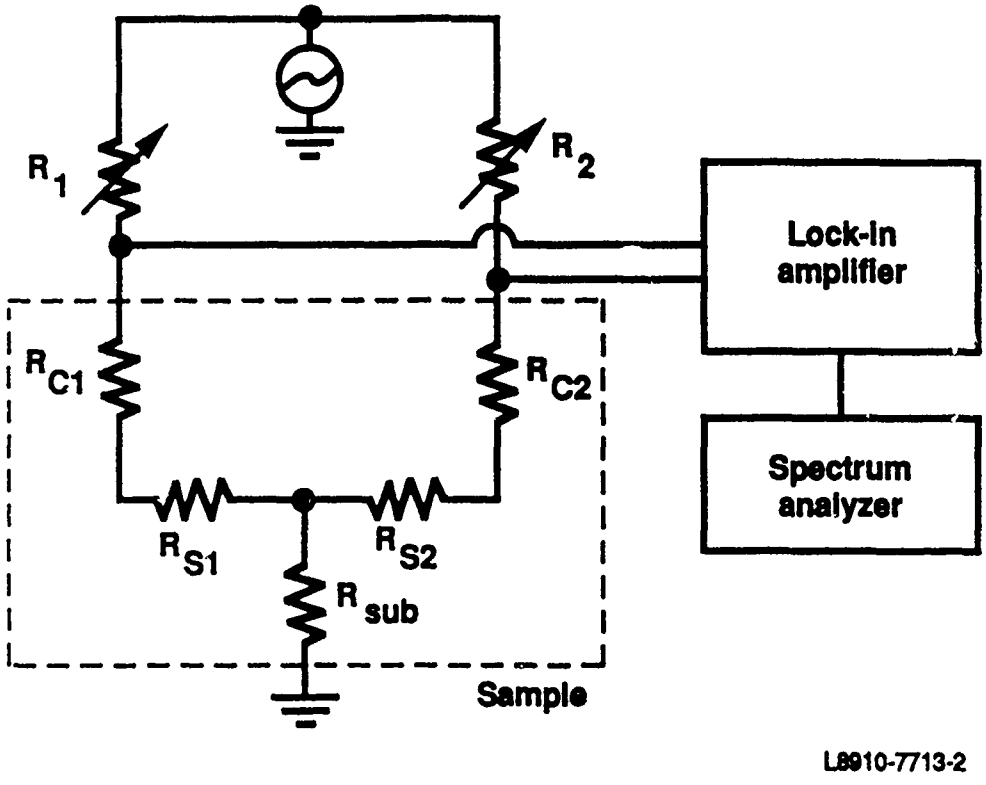

Figure 23: Bridge circuit used for low-frequency noise measurements.

the carrier to facilitate the photolithography. The samples were completed to the point of being wire bonded in their LCCs. Unfortunately, without the final funding increment, there was no time to perform the resistance and noise measurements on these samples.

B. RESULTS

Measurements of the I-V characteristics of the contacts indicated that the Au and Al contacts to $Hg_{0.79}Cd_{0.21}Te$ were ohmic, whereas the Ge contacts to $Hg_{0.7}Cd_{0.3}Te$ were partially rectifying. (A few of the gold contacts were partially rectifying.)

Figures 24–26 show the dependence of the Au, Al, and Ge contact resistance (at 300K) on contact diameter. The plotted resistances were obtained by subtracting the resistance measured between two wires attached to the substrate grid from the resistance measured between the contact and the grid. This procedure approximately cancels the resistance of the lead wires. There is considerable pad-to-pad variation in the resistances of contacts of a given size. However, for the Au and Al contacts with the lowest resistance, R, the resistance was approximately inversely proportional to the contact diameter, d, whereas for the pads with the highest resistance, the resistance was inversely proportional to d^2. These relations, which are shown as straight lines in the figures, establish an upper limit on the specific contact resistance, ρ_c and on the bulk resistivity, ρ_b. Using the expression of Cox and Strack,

$$R = \frac{4\rho_c}{\pi d_2} + \frac{\rho_b}{\pi d}\tan^{-1}\left(\frac{4t}{d}\right) \approx \frac{4\rho_c}{\pi d^2} + \frac{\rho_b}{2d} - \frac{R_\square}{4\pi}\,, \qquad (5)$$

where t is the substrate thickness and $R_\square$ is the sheet resistance of the substrate, the data implies that $(\rho_c)_{Au} \leq 9\times10^{-4}\Omega cm^2$ and $(\rho_c)_{Al} \leq 3\times10^{-3}\Omega cm^2$. The upper limits for the substrate resistivities were 6×10^{-2} Ωcm for the gold sample and 1×10^{-1} Ωcm for the aluminum sample. These are in reasonable agreement with the measured bulk resistivity of the wafer at 295K which was 5.8×10^{-2} Ωcm.

Figure 27a shows the measured noise spectrum for a pair of 100-μm-diameter Au contacts at 295K with a relatively low carrier current. Above approximately 6 Hz, the noise is composed of discrete "spikes" (presumably from residual electromagnetic or vibrational pickup) superimposed on a "white," i.e., frequency-independent, background. Below 6 Hz the noise has a clear 1/f component; the noise power actually

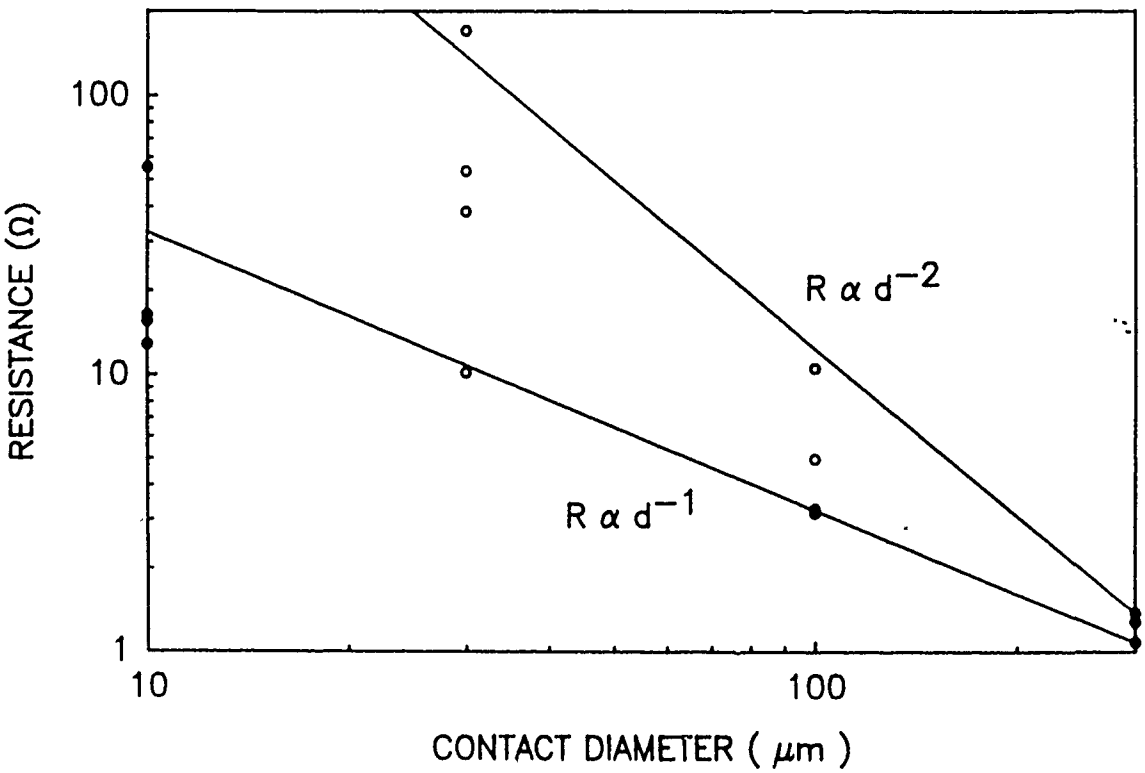

Figure 24: Contact resistance vs contact diameter for gold contacts.

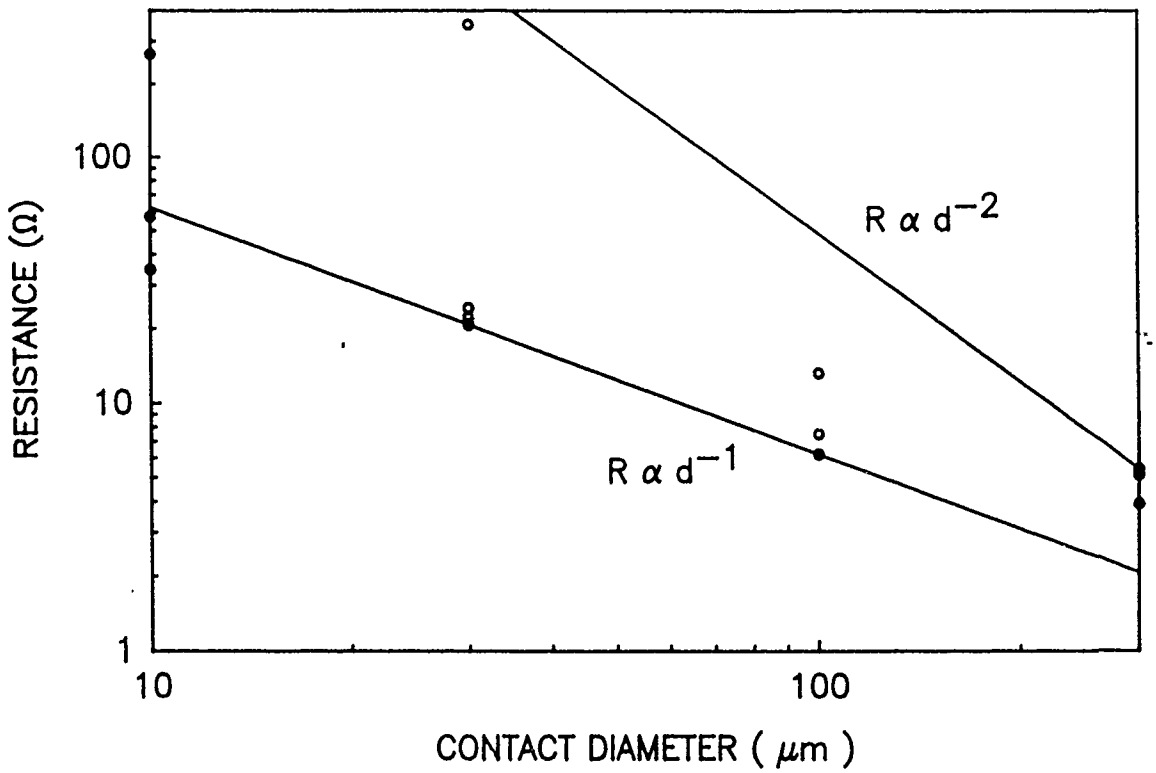

Figure 25: Contact resistance vs contact diameter for aluminum contacts.

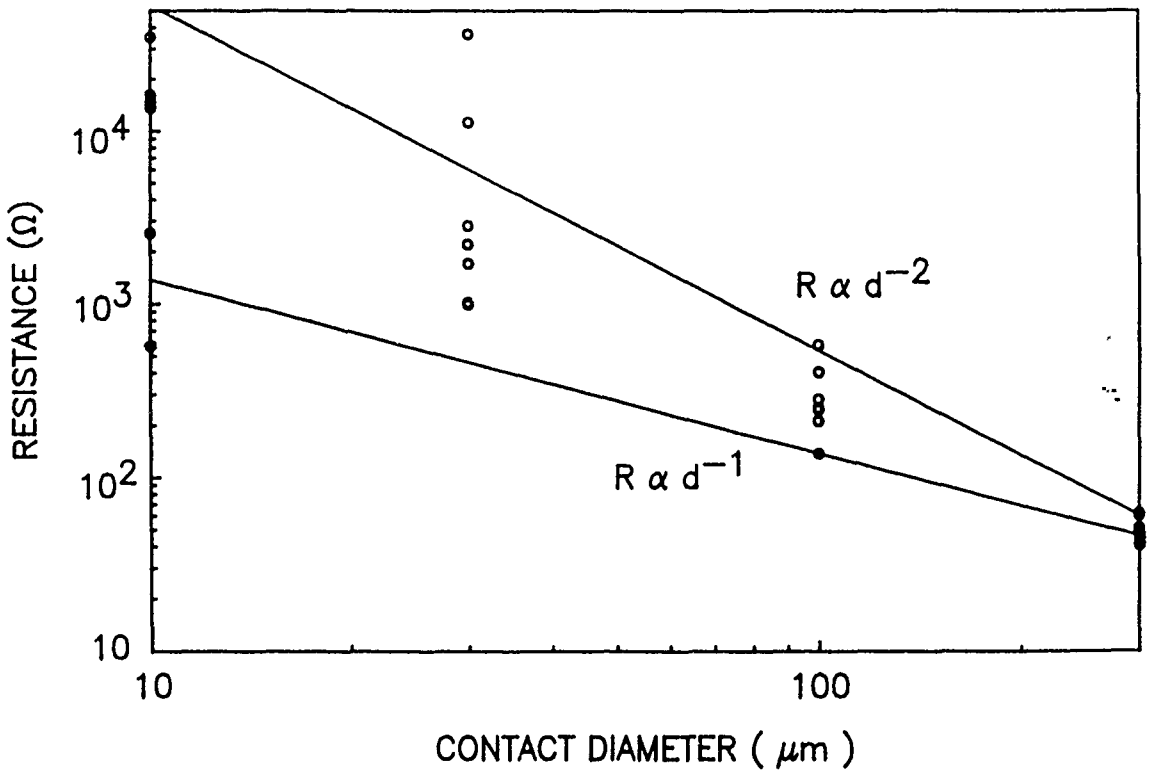

Figure 26: Contact resistance vs contact diameter for germanium contacts.

a

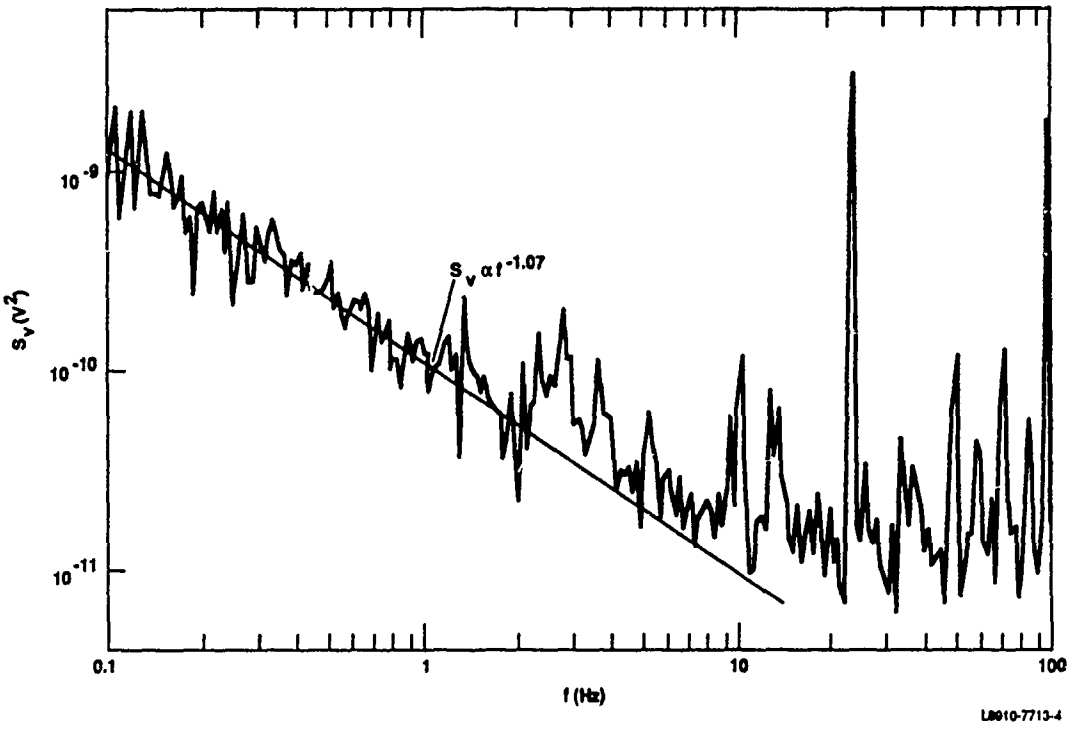

b

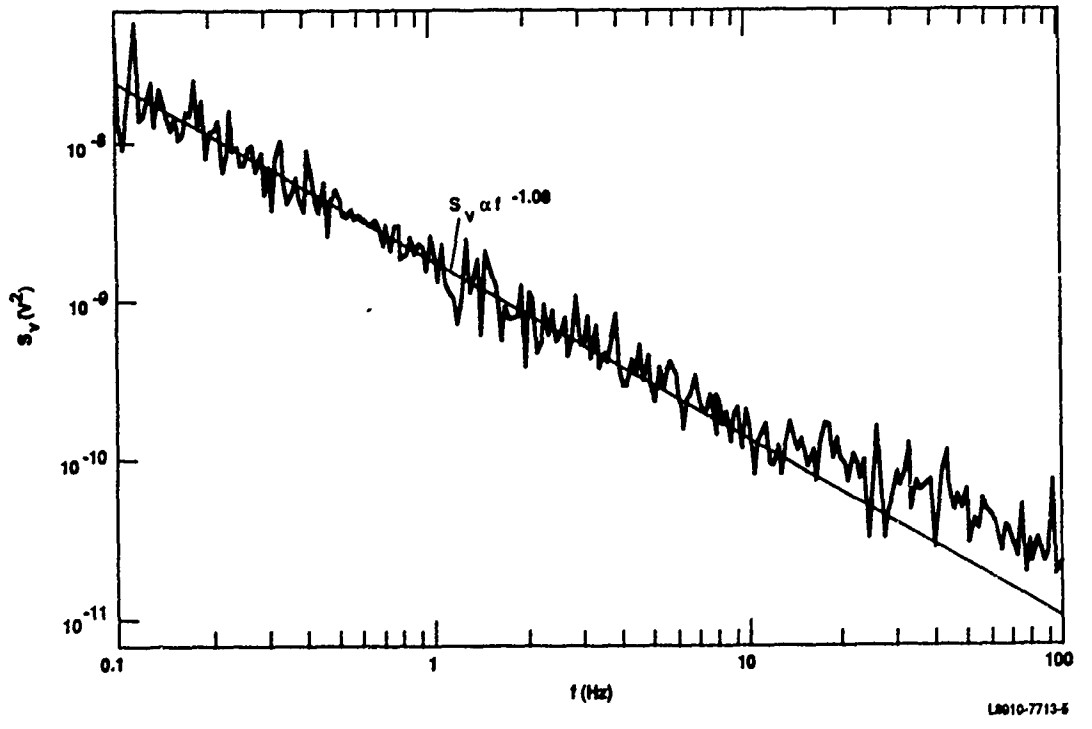

Figure 27: Noise spectrum for a pair of 10-μm-meter gold contacts with carrier current of a) 3.1×10^{-5} A and b) 3.4×10^{-4} A.

appears to be proportional to $1/f^{1.07}$. This spectrum was typical of the noise spectra seen for all of the metals at all temperatures, although the magnitude of the 1/f noise and therefore the frequency of the 1/f "knee" varied. Figure 27b shows the noise spectrum for the same pair of contacts with a larger carrier current. The "1/f" component of the noise has almost the same frequency dependence ($S_v \propto 1/f^{1.08}$) but the increase in magnitude of the noise has shifted the knee to higher frequency.

We found that the power spectral density of the voltage fluctuation, S_v, of the 1/f component was always proportional to the square of the amplitude of the ac current (I) being driven through the contact. Therefore, as is usually the case for 1/f noise, it is appropriate to express the noise as a fluctuation in the sample resistance whose power spectral density, S_R, is equal to S_v/I^2. To compare the noise from different contacts at different temperatures, we determined $S_R(100\ \text{mHz}) = [S_v(100\ \text{mHz}) - S_v(\infty)]/I^2$, where $S_v(\infty)$ is the voltage power spectral density in the high-frequency flat portion of the spectrum. Figures 28, 29, and 30 show the measured values of $S_R(100\ \text{mHz})$ as a function of the contact diameter and temperature.

C. DISCUSSION

The I-V curves demonstrate that Au and Al formed ohmic contacts to $Hg_{0.79}Cd_{0.21}Te$ whereas Ge formed partially rectifying contacts to $Hg_{0.7}Cd_{0.3}Te$. The Au and Al I-V curves remained linear down to the lowest temperature (12K) indicating that if there was a potential barrier in the regions of the contact where current flowed, it was very low or very narrow.

However, the large pad-to-pad variation in the resistance of the contacts (Figs. 24 – 26) implies a large variation in the specific contact resistance, r_c. Although r_c for some of the Au and Al contacts was low enough that the total contact resistance was limited by the substrate spreading resistance, for other contacts r_c was as high as $(\rho_c)_{Au} = 9 \times 10^{-4}\Omega\text{cm}^2$ and $(\rho_c)_{Al} = 3 \times 10^{-3}\Omega\text{cm}^2$. The large variation in r_c implies that there is an inhomogeneous potential barrier or resistive layer at the surface of the (Hg,Cd)Te.

The power spectral density of the resistance fluctuations for all three metals (S_R) was proportional to $f^{-1.1}$. The exponent of 1.1 is well within the commonly observed

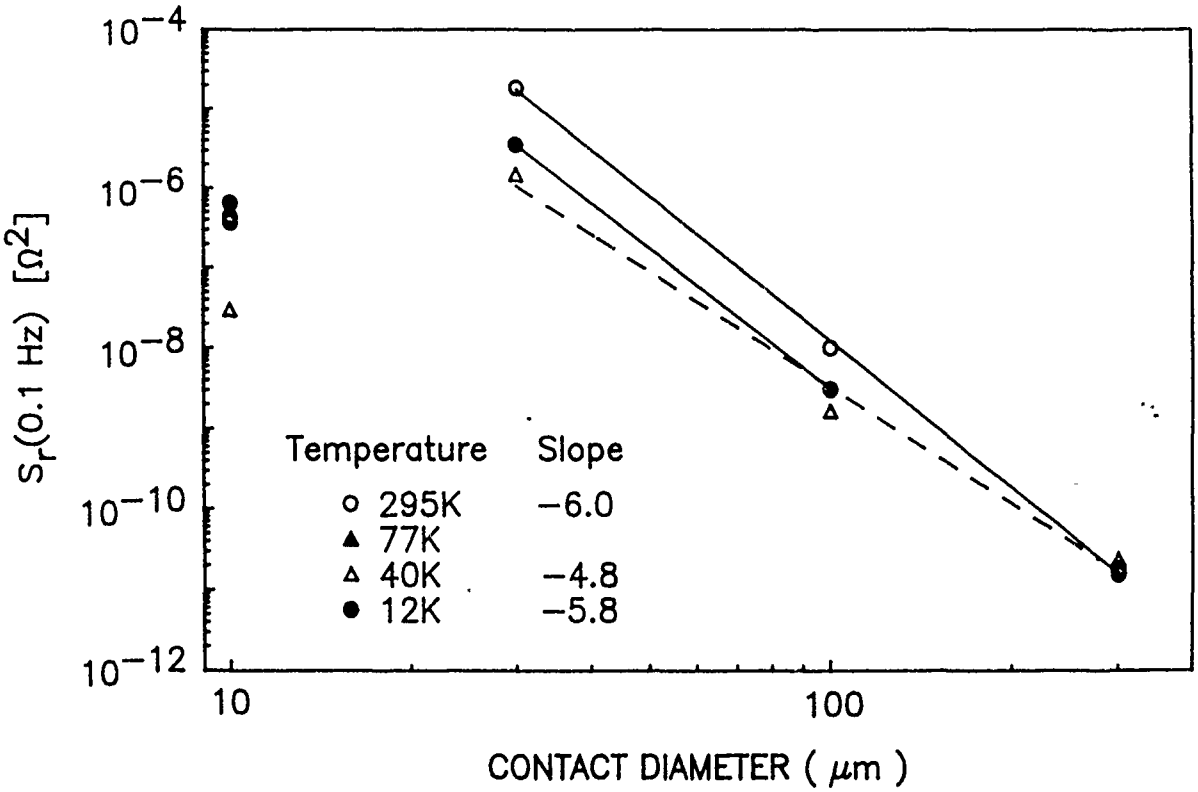

Figure 28: Power spectral density of resistance fluctuations for gold contacts.

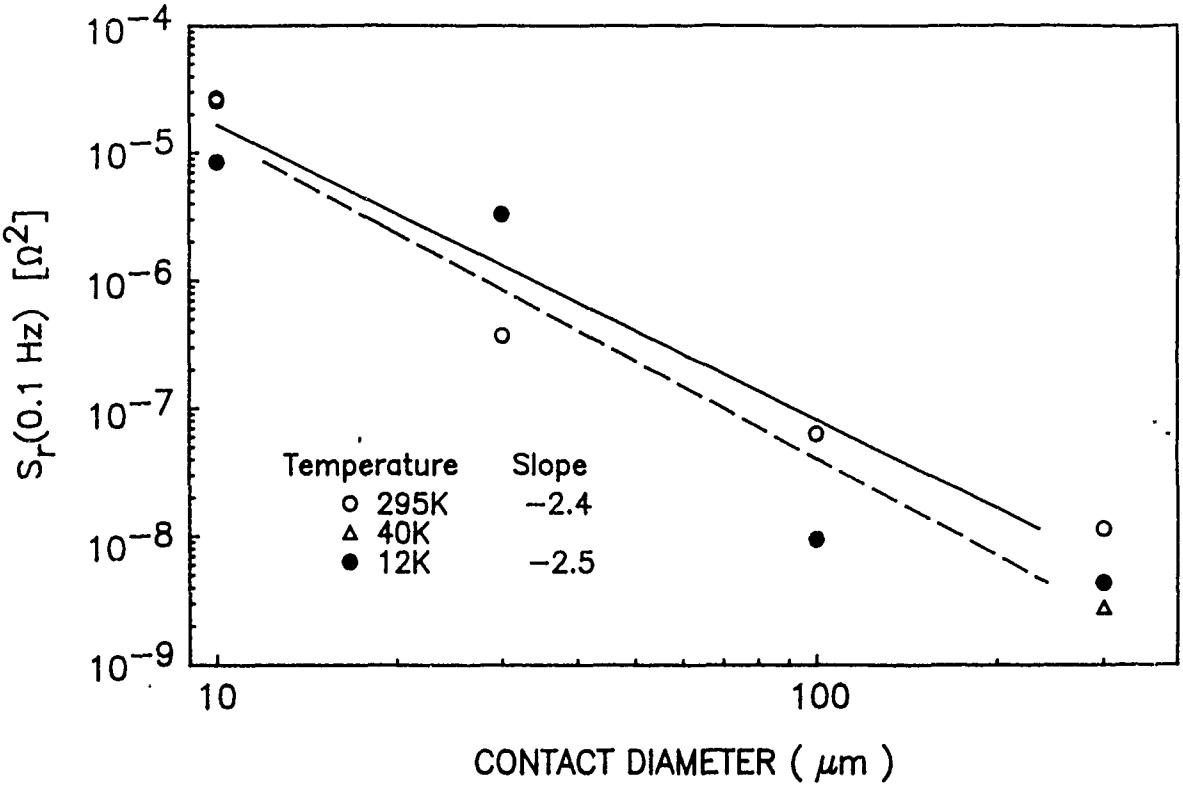

Figure 29: Power spectral density of resistance fluctuations for aluminum contacts.

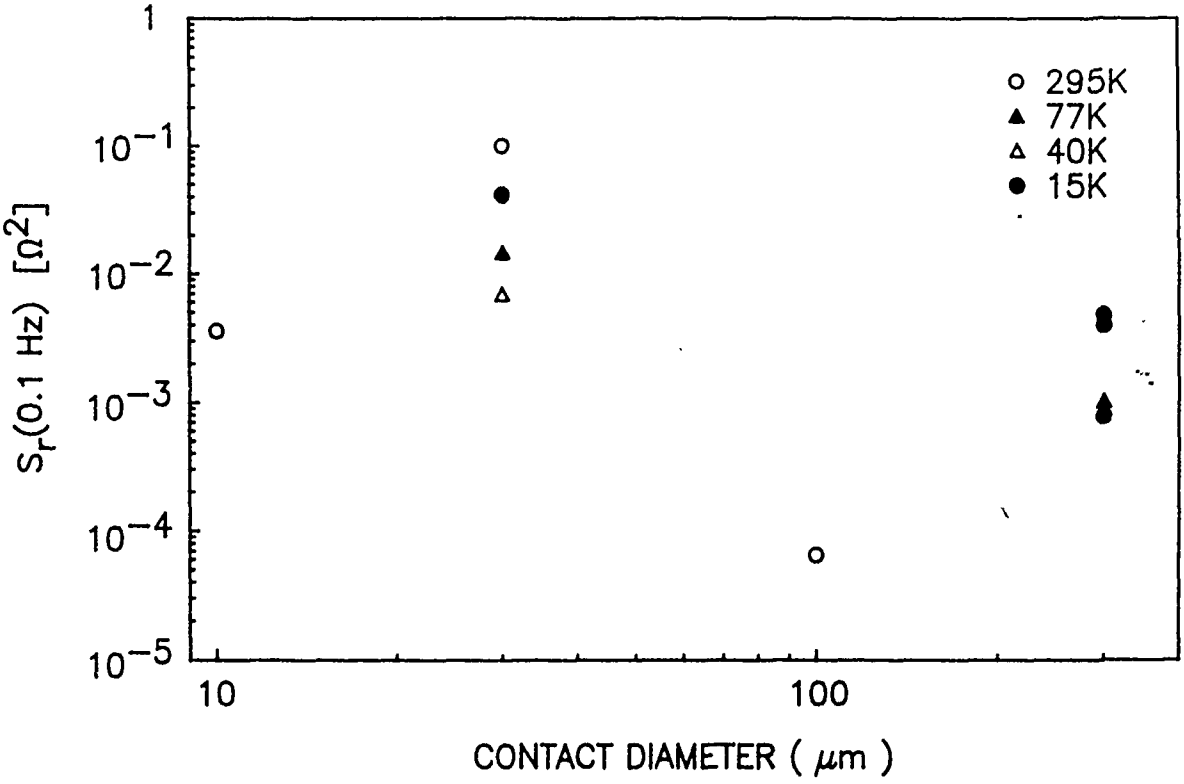

Figure 30: Power spectral density of resistance fluctuations for germanium contacts.

range of exponents for "1/f" noise. The significance of the specific value of the exponent is not yet understood.

Although the 1/f noise for the Au and Al contacts was similar for the 10-μm contacts, the dependence on contact diameter was quite different. Figure 28 shows that for the gold contacts larger than 10 μm, $S_R \propto d^{-m}$ where $5 \leq m \leq 6$. On the other hand, Fig. 29 shows that for Al, $2 \leq m \leq 3$. The value of the exponent m can be used to infer information about the current flow that generates the 1/f noise. Consider the three possible types of flow shown in Fig. 31: a) current flowing linearly away from the area of the contact (at distances $\leq$ the contact radius), b) current flowing radially away from the contact (at distances $\geq$ the contact radius), and c) lateral current in a conducting skin on the surface. By applying the Hooge equation [Eq. (1)] to thin shells which have uniform current density, we can integrate the δS_R for each shell to show that the value of the exponent m for each of these current paths is 6, 5, and 3, respectively. Therefore, we can infer that the 1/f noise from the larger gold contacts is associated with current flowing out of the area of the contact or spreading radially into the (Hg,Cd)Te, whereas the 1/f noise from the Al contacts is associated with lateral current flow along the surface (or with some other current path that decreases as slowly with distance from the contact).

If there is a conducting layer on the surface with sheet conductivity σ_{2D}, the current flowing from the contact will partially flow through the surface layer and partially through the bulk (which has conductivity σ_{3D}). The partition of the current is determined by the characteristic length, $L = \sigma_{2D}/\sigma_{3D}$; at distances $r << L$ most current flows in the surface layer, while at distances $r >> L$ most current flows in the bulk. For contacts with diameters much smaller than L, the resistance may be dominated by the surface transport. However, the 1/f noise may be dominated by the surface current even when the resistance is not, since 1) the noise is primarily generated in the region of high current density closest to the contact where the surface current is highest, and 2) the surface layer may have a higher density of traps or mobile defects than the bulk. The higher level of surface noise in the Al contacts (vs the Au contacts) could therefore be due to $(\sigma_{2D}/\sigma_{3D})_{Al} > (\sigma_{2D}/\sigma_{3D})_{Au}$ or due to a higher density of traps or mobile defects at the surface of the Al sample. Since the surface of both the Au and Al samples was sputtered to delineate the contact pads, any difference in the surfaces would have to be due to a residual effect of the metal that penetrates deeper than the depth of the ion milling (several hundred Å).

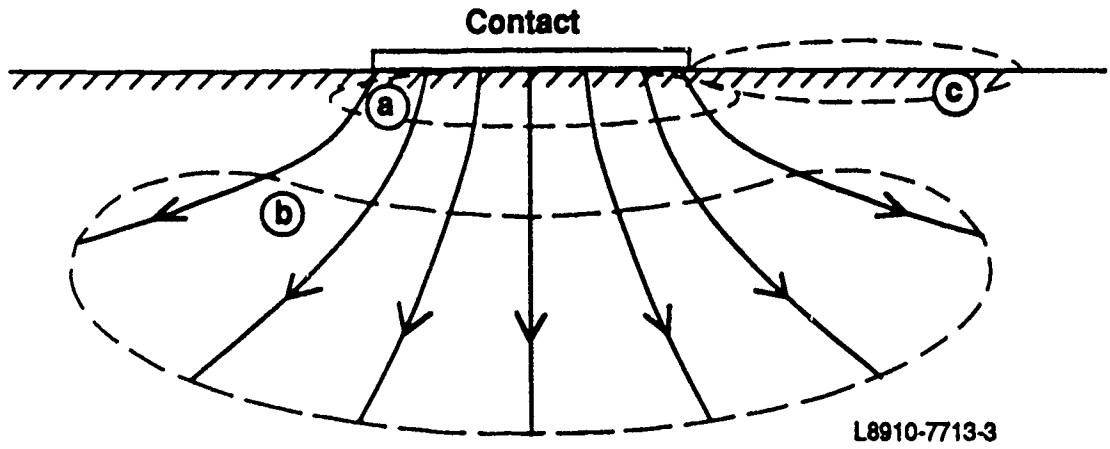

Figure 31: Regions of current flow near the contact.

We now consider whether the observed 1/f noise might be fundamental noise originating in the spreading current under the contact. By using an analysis similar to that leading to Eq. (2), it can be shown that the 1/f noise from the spreading current will be

$$S_R = \frac{\alpha_H \rho^2}{40\pi^3 n f d^5} \,. \tag{6}$$

Then, using the 295K data in Fig. 28 along with the measured wafer carrier density and resistivity we extract that $\alpha_H \approx 2 \times 10^3$. This is larger by 5 orders of magnitude than the value expected from any fundamental 1/f noise source and suggests that the 1/f noise is caused by a nonfundamental source such as traps or mobile defects near the contact. The earlier surface chemistry measurements indicated that the ion beam causes substantial depletion of Hg from the surface, and also that the Au causes outdiffusion of Te. It would therefore not be surprising if the interfacial region contained a high density of traps or other defects.

Despite the clear differences between the contacts formed by the different metals, we found no obvious correlation between the electrical properties of the contacts and their reactivity. The worst contacts (non-ohmic with high 1/f noise) were formed by Ge, which is from the intermediate reactivity group; the best contacts (ohmic with lowest 1/f noise) were formed by Au, which is unreactive. Further measurements with other metals and with vacuum-cleaved surfaces will be required to explain the observed effects.

In conclusion, all three metals showed a large variation in specific contact resistance. The Au and Al contacts were ohmic, whereas the Ge contacts were partially rectifying. The diameter dependence of the 1/f noise suggests that the noise in the Al contacts originated from a surface conduction layer near the contact, and the noise of the Au contacts originated at or below the Au/(Hg,Cd)Te interface. The magnitude of the 1/f noise indicates that it is not due to any known fundamental source and is probably related to a high density of traps or defects at or near near the contact. Although there were clear differences in the electrical properties of the Au, Al, and Ge contacts, there was no obvious relationship to the chemical reactivities. It will be useful to perform similar electrical measurements on contacts to vacuum cleaved surfaces to see if the variation in contact resistivity, r_c, and high level of nonfundamental 1/f noise are repeated or if they are caused by the ion sputtering.

IV. SUMMARY

The interactions between both cleaved and ion-sputtered (HgCd)Te and deposited overlayers were investigated and and compared to those reported by others. The overlayers were classified into four groups – ultrareactive, reactive, intermediate reactive, and unreactive – based on the relative heats of formation of the overlayer telluride and HgTe and CdTe. Ultrareactive overlayers react with both HgTe and CdTe to form an interfacial metallic telluride and elemental Hg and Cd, which are lost from the interface, whereas unreactive overlayers react only with the HgTe component. Once the HgTe is depleted from the surface region, further deposition results in growth of a metallic film. Unreactive metals, on the other hand, do not react with the surface, but form a stoichiometric interface. In contrast, the extent of interactions between intermediate overlayers and (HgCd)Te depend on other factors including the stability or reactivity of the surface and substrate material, the heats of cation alloying, and the propensity of the overlayer element to diffusion into the (HgCd)Te. The use of thin interlayers can substantially alter the interfacial behavior, however. They can either increase or decrease the indiffusion of the overlayer material into the (HgCd)Te. They can also change the overlayer morphology and control the band bending near the surface.

As a result of this program, and similar investigations by Stanford University/Santa Barbara Research Center and University of Minnesota/McDonnell Douglas, many of the chemical interactions that take place at the metal/(Hg,Cd)Te interface are now understood. The disruptions of the semiconductor stochiometry near the interface are typically very large so that with the possible exception of very unreactive metals like Ge, Au, or Sb, it is unlikely that the contacts could be described by a standard metal/semiconductor Schottky barrier model. A more realistic model would consist of metal-interlayer-semiconductor, where the interlayer probably has a different HgTe/CdTe ratio than the underlying semiconductor, a very high density of (possibly

electrically active) stochiometric defects, and possibly a high concentration of metal. However, quantitative modeling of such a structure would be very difficult, especially in light of the wide range of behaviors observed for the different metals.

The measurements of resistance and 1/f noise of Au, Al, and Ge contacts to ion-sputtered (Hg,Cd)Te demonstrated that even on a clean, uniformly sputtered surface, there can be considerable variation in the contact- specific resistance. Furthermore, 1/f noise was present in amounts far in excess of any known fundamental mechanism. The noise was likely the result of traps or mobile defects in the highly defective interlayer seen in the surface chemistry measurements. Electrical measurements on contacts to vacuum-cleaved surfaces and on contacts using other metals will be required to determine the source of the resistance variation and 1/f noise more specifically. Samples consisting of Au contacts to vacuum-cleaved material were fabricated under this program but they and additional samples to be made with the other contact metals were to be measured during the (unfunded) final six months of the program.

V. REFERENCES

[1] L.J. Brillson, Surf. Sci. Rep. **2**, 123 (1982).

[2] L.J. Brillson, J. Phys. Chem. Solids **44**, 703 (1983).

[3] G. Margaritondo, Solid-State Electronics **26**, 499 (1983).

[4] W.E. Spicer, P.W. Chye, P.R. Skeath, C.Y. Su, and I. Lindau, J. Vac. Sci. Technol. **16**, 1422 (1979).

[5] W.A. Harrison, J. Vac. Sci. Technol. A **1**, 1672 (1983).

[6] A.-B. Chen, A. Sher, and W.E. Spicer, J. Vac. Sci. Technol. A **1**, 1674 (1983).

[7] W.E. Spicer, J.A. Siberman, I. Lindau, A.-B. Chen, A. Sher, and J.A. Wilson, J. Vac. Sci. Technol. A **1**, 1735 (1935).

[8] K.C. Mills, *Thermodynamic Data for Inorganic Sulphides, Selenides, and Tellurides* (Butterworths, London, 1974).

[9] D.D. Wagman, W.H. Evans, V.B. Parker, I. Halow, S.M. Bailey, and R.H. Schumm, *Selected Values of Chemical Thermodynamic Properties*, NBS Technical Note 270, Washington, 1968.

[10] G.D. Davis, Vuoto **16**, 127 (1986).

[11] G.D. Davis, J. Vac. Sci. Technol. A **6**, 1939 (1988).

[12] G.D. Davis, W.A. Beck, Y.W. Mo,, D. Kilday, and G. Margaritondo, J. Appl. Phys. **61**, 5191 (1987).

[13] A. Wall, A. Raisanen, S. Chang, P. Philip, N. Troullier, A. Fransciosi, and D.J. Peterman, J. Vac. Sci. Technol. A **5**, 3193 (1987).

[14] D.J. Peterman, A. Raisanen, S. Chang, P. Philip, A. Wall, and A. Franciosi, J. Vac. Sci. Technol. A **6**, 1575 (1988).

[15] R.R. Daniels, G. Margaritondo, G.D. Davis, and N.E. Byer, Appl. Phys. Lett. **42**, 50 (1983).

[16] G.D. Davis, N.E. Byer, R.A. Riedel, and G. Margaritondo, J. Appl. Phys. **57**, 1915 (1985).

[17] G.D. Davis, W.A. Beck, D.W. Niles, E. Colavita, and G. Margaritondo, J. Appl. Phys. **60**, 3150 (1986).

[18] D.J. Friedman, G.P. Carey, C.K. Shih, I. Lindau, W.E. Spicer, and J.A. Wilson, J. Vac. Sci. Technol. A **4**, 1977 (1986).

[19] D.J. Friedman, G.P. Carey, I. Lindau, W.E. Spicer, and J.A. Wilson, J. Vac. Sci. Technol. B **4**, 980 (1986).

[20] D.J. Peterman and A. Franciosi, Appl. Phys. Lett. **45**, 1305 (1984).

[21] P. Phillip, A. Franciosi, and D.J. Peterman, J. Vac. Sci. Technol. A **3**, 1007 (1985).

[22] A. Franciosi, P. Phillip, and D.J. Peterman, Phys. Rev. B **32**, 8100 (1985).

[23] G.D. Davis, W.A. Beck, N.E. Byer, R.R. Daniels, and G. Margaritondo, J. Vac. Sci. Technol. A **2**, 546 (1984).

[24] G.D. Davis, W.A. Beck, M.K. Kelly, N. Tache, and G. Margaritondo, J. Appl. Phys. **60**, 3157 (1986).

[25] G.D. Davis, J.T. McKinley, D.G. Kilday, and G. Margaritondo, J. Appl. Phys. **65**, 3435 (1989).

[26] G.D. Davis, W.A. Beck, M.K. Kelly, D. Kilday, Y.W. Mo, N. Tache, and G. Margaritondo, Phys. Rev. B. **38**, 9694 (1988).

[27] G.D. Davis, W.A. Beck, M.K. Kelly, Y.W. Mo, and G. Margaritondo, Appl. Phys. Lett. **49**, 1611 (1986).

[28] D.J. Friedman, G.P. Carey, C.K. Shih, I. Lindau, W.E. Spicer, and J.A. Wilson, Appl. Phys. Lett. **48**, 44 (1986).

[29] D.J. Friedman, G.P. Carey, I. Lindau, and W.E. Spicer, Phys. Rev. B **34**, 5329 (1986).

[30] D.J. Friedman, G.P. Carey, I. Lindau, and W.E. Spicer, Phys. Rev. B **35**, 1188 (1987).

[31] G.D. Davis, W.A. Beck, D.G. Kilday, J.T. McKinley, and G. Margaritondo, J. Vac. Sci. Technol. A **7**, 870 (1989).

[32] J.M. Pawlikowski, Acta Physica Polonica **A49**, 139 (1976).

[33] J.M. Pawlikowski, Acta Physica Polonica **A49**, 563 (1976).

[34] J.M. Pawlikowski, Acta Physica Polonica **A51**, 95 (1977).

[35] J.M. Pawlikowski, Phys. Stat. Sol. (a) **40**, 613 (1977).

[36] J. Zylinski, R. Imos, and J.M. Pawlikowski, Optica Applicata **X**, 51 (1980).

[37] F.N. Hooge, Phys. Lett. A **29**, 139 (1969).

[38] A. van der Ziel, Proc. IEEE **76**, 233 (1988).

[39] P.H. Handel, Phys. Rev. Lett. **34**, 1492 (1969).

[40] P.H. Handel, Phys. Rev. B **22**, 745 (1980).

[41] S.P. Tobin, S. Iwasa, and T.J. Tredwell, IEEE Trans. Electron Devices **ED-27**, 43 (1980).

[42] W.W. Anderson and H.J. Hoffman, J. Vac. Sci. Technol. A **1**, 1730 (1983).

[43] Y. Nemirovsky, D. Rosenfeld, R. Adar, and A. Kornfeld, J. Vac. Sci. Technol. A **7**, 528 (1989).

[44] A. van der Ziel, J. Vac. Sci. Technol. A **7**, 550 (1989).

[45] G.D. Davis, Surf. Interface Anal. **9**, 421 (1986).

[46] G.D. Davis, T.S. Sun, J.S. Ahearn, and J.D. Venables, J. Mater. Sci. **17**, 1807 (1982).

[47] G.D. Davis, S.P. Buchner, W.A. Beck, and N.E. Byer, Appl. Surf. Sci. **15**, 238 (1983).

[48] U. Solzbach and H.J. Richter, Surf. Sci. **97**, 191 (1980).

[49] H.M. Nitz, O. Ganschow, U. Kaiser, L. Wiedmann, and A. Benninghoven, Surf. Sci. **104**, 365 (1981).

[50] T.S. Sun, S.P. Buchner, and N.E. Byer, J. Vac. Sci. Technol. **17**, 1067 (1980).

[51] G.D. Davis, T.S. Sun, S.P. Buchner, and N.E. Byer, J. Vac. Sci. Technol. **19**, 472 (1981).

[52] G.D. Davis, W.A. Beck, M.K. Kelly, Y.W. Mo, and G. Margaritondo (unpublished).

[53] G.P. Carey, D.J. Friedman, I. Lindau, and W.E. Spicer (unpublished).

[54] K.D. Childs and M.G. Lagally, Phys. Rev. B **30**, 5742 (1984).

[55] S. Cole, G.P. Carey, J.A. Silberman, W.E. Spicer, and J.A. Wilson, J. Vac. Sci. Technol. A **3**, 206 (1985).

[56] A. Raisanen, A. Wall, S. Chang, P. Philip, N. Troullier, A. Franciosi, and D.J. Peterman, J. Vac. Sci. Technol. A **6**, 2741 (1988).

[57] W.E. Morgan, W.J. Stec, and J.R. Van Wazer, Inorg. Chem. **12**, 953 (1973).

[58] A. Franciosi, A. Raisanen, A. Wall, S. Chang, P. Philip, N. Troullier, and D.J. Peterman, Appl. Phys. Lett. **52**, 1490 (1988).

[59] T.B. Massalski, J.L Murray, L.H. Bennett, H. Baker, Eds., *Binary Alloy Phase Diagrams* (American Society for Metals, Metals Park, OH, 1986).

[60] G.D. Davis, J. Vac. Sci. Technol. A **6**, 1939 (1988).

[61] R.H. Cox and H. Strack, Solid State Elec. **10**, 1213 (1967).

[62] J.H. Scofield, Ph. D. thesis, Cornell University, 1985.

[63] J.H.J. Lorteije and A.M.H. Hoppenbrouwers, Philips Res. Repts. **26**, 29 (1971).

VI. ACKNOWLEDGEMENTS

We gratefully acknowledge the valuable assistance of A.C. Goldberg, E. Fiore, and G. Margaritondo and his many graduate students or associates, who made many of these measurements reported here possible: E. Colavita, R.R. Daniels, M.K. Kelly, D. Kilday, J.T. McKinley, Y.W Mo, D.W. Niles, R.A Riedel, and N. Tache. We have also benefited from discussions with G.P. Carey, A. Franciosi, D.J. Friedman, D.J. Peterman, W.E. Spicer, and A. Wall. Much of the data discussed here was taken at the University of Wisconsin's Synchrotron Radiation Center, which is funded by the National Science Foundation.

We also thank John Scofield and Prof. W. Webb for demonstrating their noise measurement techniques at Cornell University.

VII. PAPERS AND PRESENTATIONS UNDER THIS CONTRACT

A. PUBLICATIONS

G.D. Davis, N.E. Byer, R.A. Riedel, and G. Margaritondo, "Interactions between cleaved (Hg,Cd)Te surfaces and deposited overlayers of Al and In," J. Appl. Phys. 57, 1915 (1985).

G.D. Davis, N.E. Byer, R.A. Riedel, and G. Margaritondo, "Deposition of Al overlayers onto cleaved (HgCd)Te surfaces," J. Vac. Sci. Technol. A **3**, 981 (1985).

G.D. Davis, "Use of surface behavior diagrams to study surfaces and interfacial reactions," Surf. Interface Anal. **9**, 421 (1986).

G.D. Davis, W.A. Beck, E. Colavita, M.K. Kelly, D.W. Niles, N. Tache, and G. Margaritondo, "Deposition of thin Al and Au overlayers onto sputtered (Hg,Cd)Te surfaces," J. Vac. Sci. Technol. A 4, 850 (1986).

G.D. Davis, W.A. Beck, D.W. Niles, E. Colavita, and G. Margaritondo, "Deposition of the reactive metals Al and In onto sputtered and cleaved Hg1-xCdxTe surfaces," J. Appl. Phys. **60**, 3150 (1986).

G.D. Davis, W.A. Beck, M.K. Kelly, N. Tache, and G. Margaritondo, "Deposition of the unreactive metal Au onto sputtered and cleaved $Hg_{1-x}Cd_xTe$ surfaces," J. Appl. Phys. **60**, 3157 (1986).

G.D. Davis, W.A. Beck, M.K. Kelly, Y.W. Mo, and G. Margaritondo, "Effect of

surface preparation on Ge overlayer growth on (HgCd)Te," Appl. Phys. Lett. **49**, 1611 (1986).

G.D. Davis, "Overlayer growth on (HgCd)Te," Vuoto **16**, 127 (1986).

G.D. Davis, W.A. Beck, M.K. Kelly, Y.W. Mo, and G. Margaritondo, "Growth of Ge overlayers onto (HgCd)Te: A comparison between cleaved and sputtered surfaces," J. Vac. Sci. Technol. A **5**, 1479 (1987).

G.D. Davis, W.A. Beck, Y.W. Mo, D. Kilday, and G. Margaritondo, "Interfacial interactions between (HgCd)Te and Ti, an ultrareactive metal," J. Appl. Phys. **61**, 5191 (1987).

G.D. Davis, W.A. Beck, M.K. Kelly, D. Kilday, Y.W. Mo, N. Tache, and G. Margaritondo, "Interactions between (HgCd)Te and overlayers of intermediate reactivity (Ag, Cu, and Ge)," Phys. Rev. B. **38**, 9694 (1988).

G.D. Davis, "Overlayer interactions with (HgCd)Te," J. Vac. Sci. Technol. A. **6**, 1939 (1988).

G.D. Davis, W.A. Beck, D. Kilday, Y.W. Mo, and G. Margaritondo, "Interfacial reactions between (HgCd)Te and intermediate reactivity overlayers," J. Vac. Sci. Technol. A **6**, 2732 (1988).

G.D. Davis, W.A. Beck, D.G. Kilday, J.T. McKinley, and G. Margaritondo, "Effects of thin interlayers on Ag/(HgCd)Te interface behavior," J. Vac. Sci. Technol. A **7**, 870 (1989).

G.D. Davis, J.T. McKinley, D.G. Kilday, and G. Margaritondo, "Effects of Al and Ti interlayers on Sb/(HgCd)Te interface behavior," J. Appl. Phys. **65**, 3435 (1989).

W.A. Beck, G.D. Davis, and A.C. Goldberg, "Resistance and 1/f noise of Au, Al, and Ge contacts to (Hg,Cd)Te," submitted to J. Appl. Phys.

B. PRESENTATIONS

"Deposition of thin Al and Au overlayers onto sputtered (HgCd)Te surfaces," G.D. Davis, W.A. Beck, E. Colavita, M.K. Kelly, D.W. Niles, N. Tache, and G. Margaritondo, 32rd Natl. Symp. Am. Vacuum Soc. (Houston, Nov. 1985).

"Interactions of metals with $Hg_{1-x}Cd_xTe$," G.D. Davis, Martin Marietta Laboratories (Baltimore, MD, March 1986).

"Effect of surface preparation on interactions of thin Cu overlayers on (HgCd)Te," G.D. Davis, W.A. Beck, M.K. Kelly, N. Tache, and G. Margaritondo, 1986 Synchrotron Radiation Center Users Group Meeting (Stoughton, WI, Oct. 1986).

"Growth of Ge overlayers onto (HgCd)Te: A comparison between cleaved and ion-sputtered surfaces," G.D. Davis, W.A. Beck, M.K. Kelly, Y.W. Mo, G. Margaritondo, 33rd Natl. Symp. Am. Vacuum Soc., 10th Int. Vacuum Congr., 6th Int. Conf. Solid Surfaces (Baltimore, MD, Oct. 1986).

"Contact formation to (HgCd)Te," W.A. Beck and G.D. Davis, ARO Workshop on Prospects for Research on Semiconductor Material Surfaces (Research Triangle Park, NC, Nov. 1986). (INVITED).

"Interfacial reactions between (HgCd)Te and intermediate reactivity overlayers," G.D. Davis, W.A. Beck, M.K. Kelly, D. Kilday, Y.W. Mo, N. Tache, and G. Margaritondo, 1987 U.S. Workshop Phys. Chem. Mercury Cadmium Telluride (New Orleans, LA, Oct. 1987).

"Overlayer interactions with (HgCd)Te," G.D. Davis, 34th Natl. Sym. Am. Vacuum Soc. (Anaheim, CA, Nov. 1987). (INVITED).

"Effects of Thin Interlayers on Ag/(HgCd)Te Interface Behavior," G.D. Davis, W.A. Beck, D.G. Kilday, J.T. McKinley, and G. Margaritondo, 35th Natl. Symp. Am. Vacuum Soc. (Atlanta, Oct. 1988).